Contract No:

This document was prepared in conjunction with work accomplished under Contract No. DE-AC09-08SR22470 with the U.S. Department of Energy.

Disclaimer:

This work was prepared under an agreement with and funded by the U.S. Government. Neither the U. S. Government or its employees, nor any of its contractors, subcontractors or their employees, makes any express or implied: 1. warranty or assumes any legal liability for the accuracy, completeness, or for the use or results of such use of any information, product, or process disclosed; or 2. representation that such use or results of such use would not infringe privately owned rights; or 3. endorsement or recommendation of any specifically identified commercial product, process, or service. Any views and opinions of authors expressed in this work do not necessarily state or reflect those of the United States Government, or its contractors, or subcontractors.

Chapter 19

The Hybrid Sulfur Cycle

Maximilian B. Gorensek, William A. Summers

Savannah River National Laboratory, Aiken, SC 29808 USA

Contents

19.1 Introduction 2

19.2 Fundamentals 4

19.2.1 SO_2-depolarized Electrolysis 4

19.2.2 High-temperature Sulfuric Acid Decomposition 9

19.2.3 Energy Considerations 11

19.3 Analytical and Experimental Studies 12

19.3.1 SO_2-depolarized Electrolyzer Component Development 13

19.3.2 Single-cell SO_2-depolarized Electrolyzer Testing 17

19.3.3 High-temperature Sulfuric Acid Decomposition 20

19.4 Process Flowsheet 23

19.4.1 Integrating a PEM SDE with a Bayonet Decomposition Reactor 24

19.4.2 The PEM SDE / Bayonet Reactor Hybrid Sulfur Flowsheet 27

19.4.3 Flowsheet Energy Requirements 35

19.4.4 Flowsheet Discussion 37

19.5 Process Engineering 39

19.6 Future Technical Challenges 45

References 47

19.1 *Introduction*

The Hybrid Sulfur (HyS) cycle (Figure 19.1) is one of the simplest thermochemical water-splitting processes, comprising only two reactions with all reactants and products in the fluid state. Known also as the Westinghouse Sulfur or Ispra Mark 11 cycle, it entails coupled reactions that cycle sulfur between its +4 (sulfite) and +6 (sulfate) oxidation states. One of the two reactions is thermochemical (high-temperature, endothermic) while the other is electrochemical, making it a hybrid thermochemical cycle.

The HyS cycle was first proposed by Brecher and Wu at Westinghouse Electric Corp. [1]. Westinghouse engineers and scientists invested considerable effort developing the cycle from its inception in the mid-1970s into the mid-1980s, publishing numerous reports [2-5], conference proceedings [6-27], papers [28-35], and patents [1, 36-37]. They referred to it as the "Westinghouse Sulfur Cycle", which explains the name by which it is still called by many. Simultaneous development also took place in Europe at the Joint Research Center in Ispra, Italy, where it was known as the Mark 11 cycle [38], and at the Nuclear Research Center (KFA) in Jülich, Germany [39-47], as well as elsewhere [48-58]. As a result of waning interest in advanced nuclear technologies beginning in the early 1980s, development activities essentially ceased. After a nearly twenty-year hiatus, interest in this process was revived following a study of thermochemical cycles that ranked HyS first among the 115 cycles considered [59]. Westinghouse resumed their investigations [60-64] and the Savannah River National Laboratory (SRNL) assumed the lead development role in the United States (US) under the Department of Energy, Office of Nuclear Energy's (DOE-NE's) Nuclear Hydrogen Initiative (NHI) [65-66]. Since then, researchers in the European Union (EU) [67], France [68-71], the Republic of Korea

(ROK) [72-73], Japan [74-82], and South Africa have also begun taking a serious look at HyS. US work on HyS has been centered at SRNL [83-102] and the University of South Carolina (USC) [103-109].

As already noted, two reaction steps are comprised in the cycle. The thermochemical step, which is common to all sulfur cycles, is the high-temperature decomposition of sulfuric acid into water, sulfur dioxide, and oxygen,

$$\mathrm{H_2SO_4}(aq) \xrightarrow{\text{Heat, T>800°C}} \mathrm{H_2O}(g) + \mathrm{SO_2}(g) + \tfrac{1}{2}\mathrm{O_2}(g)\,. \tag{19.1}$$

This is an equilibrium-limited reaction that requires a catalyst, as well as heat input at relatively high temperatures, such as those that an advanced, high-temperature gas-cooled reactor (HTGR) heat source could supply. The electrochemical step is the SO_2-depolarized electrolysis of water,

$$\mathrm{SO_2}(aq) + 2\mathrm{H_2O}(l) \xrightarrow{\text{Power, T≈80-120°C}} \mathrm{H_2SO_4}(aq) + \mathrm{H_2}(g)\,, \tag{19.2}$$

which takes place at much lower temperatures and requires electric power. Adding together the two reactions, the net effect is the splitting of one mole of water into one mole of hydrogen and one-half mole of oxygen. The same HTGR that serves as the heat source for reaction (19.1) could supply the power for reaction (19.2) with cogeneration. Power could also be used from the grid or from an independent source. The choice should be dictated by economic considerations.

The fact that the electrochemical step is an electrolysis process begs the question, why not split water directly using electrolysis,

$$\mathrm{H_2O}(l) \xrightarrow{\textit{Power}} \mathrm{H_2}(g) + \tfrac{1}{2}\mathrm{O_2}(g)\,, \tag{19.3}$$

and avoid the need to handle sulfuric acid at high temperatures? The answer lies in the much lower power requirement of the SO_2-depolarized electrolysis step, which was first proposed for

large-scale electrolytic hydrogen production by Juda and Moulton in 1967 [110]. As is well-known, the standard potential at 25°C for water electrolysis (reaction (19.3)) is -1.229V. The standard potential at 25°C for SO_2-depolarized electrolysis (reaction (19.2)), on the other hand, is only -0.158V [99]. Operating potentials are somewhat higher in both cases due to the nonstandard conditions present in real world cells and the inevitable overpotentials resulting from kinetic and mass transfer limitations, as well as Ohmic losses. Alkaline electrolyzers used to conduct reaction (19.3) typically operate at -1.8 to -2.0V, while SO_2-depolarized electrolyzers (SDEs) are expected to be capable of achieving -0.6V at practical current densities (500 mA/cm^2). Therefore, the HyS cycle requires only one-third as much electricity for the electrochemical step as conventional water electrolysis. Of course, the feasibility of the HyS cycle will depend on the sum of the primary energy required for both steps, reactions (19.1) and (19.2), being less than that required for water electrolysis, reaction (19.3).

19.2 *Fundamentals*

The two steps that constitute the HyS cycle are considered in turn, beginning with the electrochemical sulfite oxidation reaction that makes sulfuric acid and hydrogen from SO_2 and water. The high-temperature sulfate reduction reaction, which regenerates SO_2 from sulfuric acid while giving off oxygen and water, is discussed subsequently.

19.2.1 SO_2-depolarized Electrolysis

The SO_2-depolarized electrolysis step distinguishes HyS from the other sulfur cycles. Early work at Westinghouse was based on a parallel plate electrolyzer concept that used a microporous diaphragm separator. With the advent of proton exchange membranes (PEMs) such as Nafion®,

the focus shifted toward PEM designs. Nearly all of the recent SDE development has been based on PEM technology, leveraging the tremendous R&D investment for fuel cell applications.

The original patent [1] described an electrolyzer built up from parallel banks of individual cells connected in series and contained in a pressurized container. Each cell (Figure 19.2) consisted of an enclosure, 13, separated into two compartments by a membrane or diffusion barrier, 19, capable of passing protons or electrons but not sulfate or sulfite ions. An aqueous sulfurous acid (H_2SO_3) solution, 21, made by continually feeding water and SO_2 filled the cells. Both compartments held a hollow electrode equipped with a sparger, 15 and 17 (presumably for feeding SO_2), and a direct current (DC) potential of a few tenths of a V was applied between the electrode pair in each cell. Sulfuric acid was produced at the anode,

$$\mathrm{SO_2}(aq) + 2\mathrm{H_2O}(l) \rightarrow \mathrm{H_2SO_4}(aq) + 2\mathrm{H^+} + 2e^-, \tag{19.4}$$

while hydrogen gas was evolved at the cathode.

$$2\mathrm{H^+} + 2e^- \rightarrow \mathrm{H_2}(g). \tag{19.5}$$

The actual design used by Westinghouse was quite different. Sulfurous acid at the cathode is not desirable because it can be reduced to elemental sulfur or hydrogen sulfide, taking away from current efficiency, potentially poisoning the electrocatalyst, and causing other problems. High sulfuric acid concentrations in the product are desirable because they result in more energy-efficient operations downstream due to smaller quantities of water having to be vaporized by the acid concentration and decomposition processes. This led to the design shown in Figure 19.3.

Both the catholyte and anolyte contain sulfuric acid at similar concentrations (up to 75 wt % H_2SO_4) and are separately recirculated in the early Westinghouse design [2]. The anolyte feed is also saturated with dissolved SO_2. A pressure difference is imposed that forces a steady flow of acid from the cathode side to the anode side, through a microporous diaphragm separator. This is intended to counteract diffusional flux of SO_2 across the separator to the cathode. The cell is pressurized (up to 25 bar) to maximize the solubility of SO_2 in the anolyte. Hydrogen product is separated from the catholyte effluent. A portion of the anolyte effluent is removed and the unconverted SO_2 stripped off. Some of this stripped acid is fed to the cathode, enough to make up for losses across the diaphragm, while the remainder is passed on to the high-temperature decomposition step.

The development of PEM fuel cells and electrolyzers in the 1960s and 1970s led to the availability of PEM electrolyte separators, which quickly replaced the diaphragm in SDE designs. Use of membrane-electrode assemblies (MEAs) incorporating PEM electrolyte separators offered the promise of the shortest possible current path between anode and cathode, minimizing IR losses and reducing the SDE footprint. Much of the early HyS work was focused on identifying PEM formulations that had good conductivity (low resistance) at high H_2SO_4 concentrations together with low SO_2 permeability [4, 44].

Figure 19.4 illustrates the SDE configuration used by SRNL. The MEA (anode catalyst layer, PEM, and cathode catalyst layer) is at the “heart” of the SDE. A carbon cloth or paper diffusion layer is pressed against each side by a graphite flow field which is designed to force fluid flow through the diffusion layer. The anolyte is sulfuric acid saturated with dissolved SO_2. Unlike the

Westinghouse design, the catholyte is water. This helps the membrane remain hydrated and also serves to sweep out any elemental sulfur that may form at the cathode due to SO_2 crossover. SO_2 reacts with water at the anode to form sulfuric acid, protons, and electrons according to reaction (19.4). The protons pass through the PEM under an applied potential and recombine with the electrons at the cathode to make hydrogen via reaction (19.5). Essentially no undissociated H_2SO_4 remains in solution at typical anolyte concentrations, 30-75 wt % H_2SO_4. (Experimental measurements and thermodynamic analyses have shown that nearly all of the sulfuric acid is present as sulfate and bisulfate ion under these conditions [111-116].) Consequently, both the applied potential and the anionic character of the membrane provide an effective barrier to sulfate and bisulfate ion diffusion, keeping sulfuric acid out of the catholyte. More details concerning the SRNL SDE are given below.

The use of a PEM imposes some limitations on the SDE. The conductivity of the most common PEM material, Nafion®, depends on the water content of the membrane; water content, in turn, depends on the activity of water at the membrane surfaces. When in contact with sulfuric acid, it has been shown that the resistivity of Nafion® increases with the H_2SO_4 content of the acid. The practical upper limit for the acid concentration in a Nafion®-equipped SDE is about 50 wt % H_2SO_4 [95]. To achieve higher acid product concentrations will require using a PEM other than Nafion® – preferably one that has good conductivity and low SO_2 permeability at high acid strength [109]. Furthermore, Nafion® is limited to an operating temperature less than 100°C. Use of a PEM that can operate at higher temperatures is one way to improve the reaction kinetics and increase the electrolyzer efficiency.

Recirculation of the anolyte and catholyte in the SRNL SDE design serves several purposes. On the anolyte side, flow through the porous flow field helps increase mass transfer, including transport of dissolved SO_2 from the bulk solution to the anode surface as well as removal of H_2SO_4 product from the anode surface to the bulk phase. Furthermore, anolyte recirculation is inevitable due to SO_2 solubility and conversion limitations. On the cathode side, the flow of water helps sweep hydrogen bubbles from the cathode surface and keeps the membrane hydrated. It also removes any sulfur fines that can build up due to the reduction of any SO_2 that diffuses across the PEM from the anode. In the full-scale plant, recirculation of both flows through heat exchangers will be used to help control temperature and recover waste energy from the electrode overpotentials and Ohmic losses in the form of heat to use elsewhere in the cycle.

An alternative SDE design was concurrently developed and tested at USC [103]. As illustrated in Figure 19.5, gaseous SO_2 is fed to the anode while liquid water is fed to the cathode, which is maintained at a higher pressure than the anode. This pressure differential drives a net water flux across the PEM and keeps it hydrated. Water transported across the membrane reacts with gaseous SO_2 at the anode to make sulfuric acid, which accumulates and is removed as the anode product. When compared to the all-liquid SRNL design, a significantly higher catholyte (water) recirculation rate will be needed in order to control the SDE temperature. More importantly, a HyS flowsheet incorporating this gaseous anode design will differ in the way the products of the high-temperature sulfuric acid decomposition step are handled in order to produce a gaseous SO_2 feed to the anode instead of a sulfuric acid feed containing dissolved SO_2. Since SO_2 and O_2 are quite easily separated based on their solubility difference, the gaseous SO_2 anode flowsheet will be somewhat more complex because it can't use simple preferential dissolution to do this separation.

Otherwise, the performance of this design is expected to be comparable if the same PEM and electrode materials are used.

19.2.2 High-temperature Sulfuric Acid Decomposition

As noted earlier, the high-temperature decomposition of sulfuric acid into water, sulfur dioxide, and oxygen, reaction (19.1), is common to all sulfur cycles. Consequently, this topic has already been addressed at length as part of the Sulfur-Iodine (SI) cycle. However, several aspects of relevance to HyS are worth mentioning here.

In their second-law analysis of the HyS cycle, Knoche and Funk [58] showed that the net thermal efficiency is limited by the temperature range over which heat is exchanged between the primary energy source (the HTGR) and the water-splitting process, among other things. This is true for any heat-driven water-splitting process. The higher the HTGR coolant outlet temperature and the smaller the difference between the outlet and inlet temperatures, the higher the reversible or limiting efficiency will be. Thus, it is clear that the design of the high-temperature step of the HyS cycle will have a significant impact on the performance of the overall process.

A generic schematic of the way in which high-temperature heat would be transferred from the HTGR to the HyS process is illustrated in Figure 19.6. The primary coolant is assumed to be helium under pressure (40-90 bar). Indirect heating by means of a secondary helium loop will be inevitable for isolation purposes. This is accomplished by means of an intermediate heat exchanger (IHX). The process heat exchanger in the HyS cycle is the acid decomposition reactor, which will achieve a peak process fluid temperature about 75°C lower than the reactor outlet

temperature. As the coolant temperature decreases, additional heat may be transferred to an acid vapor superheater or acid vaporizer (not shown). Depending on the HTGR design, the coolant return temperature may be too low for all of the heat to be used for sulfuric acid decomposition. In that case, steam may also be made, as shown in Figure 19.6, for a bottoming power cycle or heating needs elsewhere in the process.

Early flowsheets proposed by SRNL [83, 86] featured a high-temperature sulfuric acid decomposition process design adapted from one proposed by Öztürk et al. [117] for the SI cycle. The key feature was a direct contact heat exchanger/sulfuric acid scrubber as shown in Figure 19.7. This scrubber served as a sulfuric acid trap since the total vapor overhead product could only contain very small amounts of H_2SO_4 due to the highly nonideal behavior of the H_2O-H_2SO_4-SO_3 system. Consequently, it offered the promise of high thermal efficiency since essentially all of the liquid H_2SO_4 fed would be converted to SO_2 vapor. A simple energy balance then shows that the high-temperature heat requirement would be equal to the enthalpy difference between the SO_2-O_2-water vapor product stream and the liquid acid feed stream. For fully converting an equimolar H_2O-H_2SO_4 liquid feed (84.5 wt % H_2SO_4) to an H_2O-SO_2-O_2-vapor product stream at 300°C and 12 bar, the enthalpy difference would only be 317 kJ/mol SO_2 (a low value representing high efficiency).

However, Moore et al. [118] cited serious corrosion problems and difficulties in making and maintaining the high-temperature connections required for this design. As a result, they abandoned the direct contact heat exchanger/sulfuric acid scrubber approach in favor of a recuperative bayonet reactor for the NHI Integrated Laboratory Scale (ILS) SI cycle

demonstration. [118] A simplified schematic of this design is shown in Figure 19.8. (While the ILS unit actually used electrical resistance heaters on the outer surface, the full-scale reactor would be heated by secondary helium coolant flowing past the exterior.) The bayonet reactor embodies all of the operations shown in Figure 19.7 in a single unit, albeit without direct contact heat exchange and requiring only two fluid conduit connections (inlet and outlet) at much lower temperatures. A detailed analysis by Gorensek and Edwards [98] indicates that the energy requirements could be low enough to be incorporated in a practical HyS process that would compare favorably with water electrolysis. Consequently, the bayonet reactor was chosen as the basis for subsequent SRNL HyS flowsheets [95, 97].

19.2.3 Energy Considerations

The HyS process will be practical as a means for producing hydrogen from nuclear energy only if it will cost less to do so than by alternate means. The obvious benchmark is nuclear water-splitting by alkaline electrolysis using electricity from a nuclear power plant. Unless HyS has the potential to make hydrogen at a lower total cost, there is no reason to pursue its development any further. After all, the technology to make electricity with a pressurized water reactor (PWR) or boiling water reactor (BWR) and use that power to drive an array of alkaline electrolysis cells to make hydrogen is already well-established.

Arguably the most expensive component of a hydrogen production process driven by nuclear energy would be the nuclear reactor heat source. This implies that the net thermal efficiency of a nuclear water-splitting process is a key discriminator. If one process has significantly higher efficiency than another, it is likely to cost less. For example, if a HyS plant had a net thermal

efficiency of 45% compared to an alternative plant with 30% efficiency, this would mean that only two reactors would be needed to produce the same quantity of hydrogen using the HyS process that would require three reactors with the alternative process.

The electrical generating efficiency for a typical BWR/PWR power plant is approximately 33%, while alkaline electrolysis can make hydrogen from electricity with a lower heating value (LHV) efficiency of about 68%. This gives a net thermal efficiency of 22.4% (LHV basis) for nuclear-powered electrolysis [95]. Of course, if HTGRs are available for hydrogen production, they could be used to generate electricity too. The conversion efficiency for an HTGR-heated closed loop helium Brayton power cycle has been projected to range between 41% [119] and 52% [120], depending on the design and underlying assumptions. Taking 45% as a conservative estimate, using HTGR power would give alkaline electrolysis a net thermal efficiency of 30.6% (LHV basis) [95]. For a HyS process to be practical, it must exceed these efficiency benchmarks by a considerable margin. As discussed in Section 19.4, SRNL has devised process flowsheets that demonstrate the potential of a HyS process to achieve acceptable efficiencies.

19.3 *Analytical and Experimental Studies*

Of the thermochemical and hybrid cycles, only the SI has been more extensively studied than the HyS cycle. SDE component development efforts will be addressed first, followed by a review of electrolyzer testing results. This section will conclude with a discussion of high-temperature sulfuric acid decomposition reactor developments, which are, for all practical purposes, shared with the SI cycle.

19.3.1 SO_2-depolarized Electrolyzer Component Development

The SDE is composed of several major components, each of which requires careful selection, analysis, characterization, and experimental study. The use of a PEM as the cell electrolyte dictates the general geometry and design approach for the SDE. A schematic showing the major components of a PEM-type SDE is given in Figure 19.9. Experimental study at the component level has primarily focused on the PEM electrolyte and the electrocatalyst for both the anode and cathode.

Selection of a suitable catalyst is important in order to 1) increase the electrical efficiency by minimizing kinetic overpotential losses and allowing the SDE to operate at conditions closer to the reversible cell potential, and 2) maintain long-term stable cell performance. Prior work by Westinghouse Electric in the 1980s investigated the use of precious metal blacks (Pd and Pt) as electrocatalysts for the SDE reactions [4]. The results indicated that palladium was a more effective electrocatalyst than platinum for SO_2-depolarized electrolysis. More recently, SRNL conducted experimental work to compare high surface area catalysts using palladium on carbon (Pd/C) and platinum on carbon (Pt/C) [91].

The catalyst activity and stability were evaluated using a three-electrode cell consisting of a glass vial with a Teflon cap and a water jacket. Electrochemical characterization of catalysts consisted of cyclic voltammograms (CVs) in the solution purged with nitrogen and linear sweep voltammograms (LSVs) in SO_2-saturated sulfuric acid solutions. The catalytic activity and stability of Pt/C and Pd/C were studied in 3.5–10.4 M (30-70 wt %) sulfuric acid solutions and at temperatures ranging from 30 to 70°C. The results are shown in Figure 19.10 [91]. Pd/C showed

somewhat higher initial activity than Pt/C, but was much less stable. After a few cycles, the activity of the Pd/C catalyst decreased significantly, whereas the Pt/C exhibited very good stability and activity for the oxidation of SO_2. Pt/C did exhibit instability in very high H_2SO_4 concentrations (10.4 M) at temperatures of 50°C and above. Tafel plots showed lower potentials (ca. 100 mV) and much higher exchange currents (ca. 1000 times greater) for the oxidation of SO_2 on Pt/C compared to Pd/C. Furthermore, the activation energy for the oxidation of SO_2 on Pt/C is at least half of that on a Pd/C surface. As a result, SRNL focused its SDE work on the use of Pt electrocatalysts.

Experiments were also carried out by SRNL to measure the performance of Pt-alloy catalysts created by alloying Pt with various transition metals [101]. The potential vs. current relationship is shown in Figure 19.11 [101] in the form of Tafel plots. As shown there, when the potential approaches the open circuit potential and the exchange current density, it varies, depending on the transition metal that is alloyed with the Pt. It is interesting to note that the best performance is observed when Pt is alloyed with non-noble metals such as cobalt and chromium. Note, however, that when Pt is alloyed with noble metals such as iridium or ruthenium, the performance is decreased. The best performance was measured with a catalyst featuring Pt alloyed with Co and Cr. This catalyst produced a 20-mV decrease in the potential compared to the baseline Pt/C catalyst. However, a further decrease in the potential is needed to achieve the commercial performance target. Thus, there is a need to further increase the anode catalyst performance for the oxidation of sulfur dioxide. This can be accomplished through a combination of more active catalysts and increased operating temperature, which improves the overall kinetics.

In addition to the electrocatalyst, the other key component of an SDE is the PEM electrolyte. There are many requirements of a PEM for the successful functioning of the electrolyzer. The PEM must be stable in highly corrosive solution (>30 wt % H_2SO_4 saturated with SO_2) and at high operating temperature (80 to 140°C), allow minimal transport of SO_2, and must maintain high ionic conductivity under these conditions. These requirements allow the electrolyzer to perform at high current density and low cell potential, thus maximizing the energy efficiency for hydrogen production. Lastly the PEM serves to separate the anolyte from the hydrogen output in order to prevent the production of undesired sulfur-based reaction products and poisoning of the cathode catalyst.

The SRNL has investigated numerous candidates for use as membranes in the SDE [93]. Both commercially-available and experimental membranes were selected and evaluated for chemical stability, sulfur dioxide transport and ionic conductivity characteristics. An array of thicknesses, equivalent weights, chemistry, and reinforcements were considered. Commercial membranes included perfluorinated sulfonic acid (PFSA) membranes, such as DuPont Nafion® series, which is widely used in PEM fuel cells. Nafion® series membranes exhibited excellent chemical stability and ionic conductivity in sulfur dioxide-saturated sulfuric acid solutions. Sulfur dioxide transport in these membranes varied proportionally with the thickness and equivalent weight of the membrane. Although the SO_2 transport was higher than desired, the excellent chemical stability and conductivity indicated this membrane type as the best commercially-available membrane at this time. The Nafion® series membranes were therefore chosen as the benchmark for comparing membrane performance.

Many of the membranes considered are also being utilized or are under development for use in PEM fuel cells, PEM electrolyzers and/or direct methanol fuel cells (DMFCs). This permits the developers of an SDE to leverage much of the extensive work being done by others for these related PEM applications. Membranes being developed for DMFC applications are particularly relevant, since a major challenge for this technology is the reduction of methanol crossover. Methanol, like sulfur dioxide, is a neutral species that is soluble in water. The methanol crossover issue is similar to the SDE problem with the crossover of dissolved SO_2. A list of some of the membranes selected and characterized by SRNL is given in Table 19.1. All of these membranes exhibited excellent short term chemical stability in concentrated sulfuric acid solutions at temperatures up to 80°C.

The conductivity and SO_2 transport for each membrane were evaluated using a custom-made permeation cell consisting of two glass chambers joined by a Teflon™ bridge where the membrane is secured. During measurements both chambers were filled with the concentrated acid of interest (typically 30 wt % H_2SO_4) and purged of oxygen by flowing nitrogen. A constant potential was applied and the SO_2 transport through the membrane was determined by measurement of the current as a function of time. Each membrane was also tested for through-plane ionic conductivity using electrochemical impedance spectroscopy. Representative results are shown in Figure 19.12 [93].

The lowest SO_2 transport coefficient was measured for membranes of the DuPont bilayer and high equivalent weight PFSA type. However, these membranes also showed unacceptably low ionic conductivity, negating their use in the SDE. Several of the advanced membranes had promising

combined performance (low SO_2 transport and high conductivity). Both the PFSA/FEP blend and the BPVE-6F membranes exhibited lower SO_2 transport than Nafion®, but with somewhat lower ionic conductivity. The SDAPP membrane had high conductivity, but also a somewhat higher SO_2 transport coefficient. Results for the PBI membrane (not shown in Figure 19.12) were also encouraging, with low SO_2 transport and reasonable conductivity.

The reported test results were determined at 67°C and atmospheric pressure. However, several of the more promising membranes, such as the PBI, Clemson BPVE and Sandia SDAPP, are expected to perform significantly better at higher temperature (120-140°C), which is not possible with the PFSA membrane. The higher temperature operation is also expected to improve reaction kinetics and lower the cell potential. Preliminary testing of these membranes at higher temperature using anhydrous SO_2 as the anolyte has shown promising results [105]. Operation with liquid anolyte (SO_2 dissolved in sulfuric acid) at the higher temperature requires a higher pressure test facility in order to maintain adequate SO_2 concentrations in the feed. No results for higher-temperature/higher-pressure testing with a liquid-fed SDE have been reported yet, although this is an obvious future research direction.

19.3.2 Single-cell SO_2-depolarized Electrolyzer Testing

Previous electrolyzer tests using SO_2 depolarization were reported by Westinghouse in the 1970s [4, 20, 28]. More recent tests have been reported by USC [104-109] and SRNL [85, 89, 100]. As discussed previously, Westinghouse employed a two-compartment filter-press type cell rather than the more compact fuel cell-type PEM arrangement used by current investigators. The USC tests employed a 10-cm^2 cell based on conventional PEM architecture. Liquid water was fed to the

cathode and gaseous SO_2 was fed to the anode. A Nafion® membrane electrode assembly (MEA) using Pt black catalyst on both the anode and cathode was employed. Polarization curves for Nafion® membranes N212, N115, and N117 are shown in Figure 19.13 [104]. These membranes have thicknesses of 51, 127 and 178 μm, respectively. A differential pressure of 600 kPa across the membrane (higher on the cathode) and an operating temperature of 80°C were maintained. The thinner membranes have lower cell potentials and permit higher current densities. At a current density of 500 mA/cm^2, the N212 cell achieved a cell potential of 720 mV. The measured sulfuric acid concentration leaving the cell was 4.2 M. However, the thinner membranes are also expected to permit more SO_2 crossover from the anode to the cathode. Furthermore, the authors concluded that Nafion® membranes were not a suitable choice for an SDE due to the significant reduction in conductivity in the presence of concentrated sulfuric acid. Alternatively, they recommended the development of a novel PEM in which the conductivity is not adversely affected by sulfuric acid.

Extensive SDE testing has been reported by SRNL using both a button-cell electrolyzer and a larger single-cell electrolyzer. Photographs of the single cell electrolyzer are shown in Figure 19.14. It is constructed of steel support plates, graphite plates, graphite flow fields, graphite diffusions layers, PVDF gaskets and PFA-lined steel tubing. Copper current collectors are sealed from contacting the process fluids. The cell is designed to permit easy replacement of the MEA, consisting of the PEM bonded between platinized carbon anode and platinized carbon cathode layers. The cell has a nominal active cell area of 60 cm^2. A test facility capable of automated unattended testing of SDE units at pressures up to 600 kPa and temperatures up to 80ºC was designed and constructed. Most of the single-cell tests were operated to generate approximately 10-20 L/hr of hydrogen. The SDE was operated in the liquid-fed mode, with the anolyte consisting

of sulfuric acid saturated with dissolved sulfur dioxide. Water was also added on the cathode side of the cell in order to maintain membrane hydration and to remove any sulfur species that could result from SO_2 crossover.

Thirty-seven different MEA configurations were tested, with representative polarization curve results shown in Figure 19.15 [94]. The test results show a cell potential of approximately 760 mV at a current density of 500 mA/cm^2 during operation at 80°C with 30 wt % sulfuric acid. Operation at higher temperature (120-140°C) and use of advanced membranes are expected to lower the cell potential to a value nearer the commercial goal of 600 mV at 500 mA/cm^2. The advanced membranes will also be required to maintain high conductivity in the presence of high sulfuric acid concentrations.

A major concern of SDE operation is the diffusion of sulfur dioxide through the PEM to the cathode where it can be reduced to hydrogen sulfide and eventually elemental sulfur. Earlier tests performed by SRNL revealed the build-up of a sulfur layer inside of the cell's MEA [96]. More recent testing indicated that such a sulfur build-up could be avoided through the proper selection of membranes and the choice of operating conditions. In this case, the SO_2 crossover may be reduced to the point where a manageable amount of H_2S (part-per-million level) is generated and leaves the cell with the hydrogen gas, but no sulfur build-up occurs inside the SDE. SRNL conducted two tests of 212 hours each using a Nafion® membrane verifying this mode of operation [102]. Longer term testing is planned in the future, including operation at higher temperature and pressure using advanced membranes.

SRNL has also demonstrated multi-cell SDE stack operation [92]. A photograph of a three-cell SDE installed in the SRNL test facility is shown in Figure 19.16 [92]. This unit utilized round plates with 160 cm^2 active area per cell stacked in a bipolar arrangement. It was successfully operated at 80°C and 700 kPa for 72 hours with a constant hydrogen output of 86 L/hr. Development of higher capacity SDE units, consisting of larger area plates in multi-cell stacks, will be necessary in order to construct commercial-scale electrolyzers.

19.3.3 High-temperature Sulfuric Acid Decomposition

The decomposition of sulfuric acid to release oxygen and regenerate sulfur dioxide is the thermochemical step in the HyS cycle. It is also the high-temperature step of the SI thermochemical cycle. Much of the research and testing for this step has been performed as part of the work on the SI cycle, and it can mostly be directly applied to HyS. Therefore, in order to minimize redundancy, the reader is referred to the section of this book regarding the SI cycle for a review of the analytical and experimental studies of high temperature sulfuric acid decomposition. However, a recent analysis of the bayonet design concept for sulfuric acid decomposition [98] will be briefly reviewed here.

The recuperative bayonet reactor design was evaluated using pinch analysis in conjunction with statistical methods. The primary objective was to establish the minimum energy requirements without having to perform a detailed heat transfer design. This meant calculating the minimum heating target, or the lowest possible heat input if all thermodynamically feasible recuperation were to be fully utilized. Another objective was to determine the heating utility pinch temperature for the helium heat transfer fluid, i.e. the lowest temperature to which the secondary helium loop

could be cooled by heat exchange with the bayonet without establishing inefficient, cross-pinch heat transfer. Aspen Plus [121] and Aspen Energy Analyzer [122] were used for the bayonet reactor simulations and pinch analyses, respectively, while JMP [123] was used to suggest simulation "experiments" and perform statistical analyses of the results.

The lowest value of the minimum heating target, 320.9 kJ/mol SO_2, was found at the highest pressure (90 bar) and peak process temperature (900°C) considered, and at a feed concentration of 42.5 mol% H_2SO_4. This assumed a 10°C minimum temperature difference for recuperation, a catalyst bed inlet temperature of 675°C, and local attainment of the decomposition equilibrium in the catalyst bed. Feed temperature was found not to affect the heating target.

For the overall HyS process to be competitive with PWR/BWR-powered alkaline electrolysis, it has been shown that the acid decomposition step should consume no more than about 450 kJ/mol SO_2 (which would provide a 33% net thermal efficiency advantage) [95]. This means that the bayonet design is capable of achieving a heating requirement low enough for a HyS water-splitting process that should be able to compete with electrolysis, even taking into account the additional energy needed to concentrate the acid feed.

Above 800°C peak process temperature, lower pressure gave higher heating targets, while the effect was reversed below 800°C. Lower temperatures consistently gave higher minimum heating targets. This behavior is illustrated in Figure 19.17 [98]. The lowest peak process temperature that could meet the 450-kJ/mol SO_2 benchmark turned out to be 750°C (allowing up to 75 kJ/mol SO_2 for preconcentration of the acid feed), although operation at a pressure significantly lower than that

of the helium heat transfer fluid would be required. If the decomposition reactor were to be heated indirectly by an advanced gas-cooled reactor heat source with a 50°C temperature difference between the primary and secondary coolant loops, and a 25°C minimum temperature difference between the secondary coolant and the process, then a HyS cycle using the bayonet concept could be competitive with alkaline electrolysis provided the reactor outlet temperature is at least 825°C, preferably higher. The bayonet design will likely not be practical for use with reactor outlet temperatures below 825°C. In this case, a design based on the direct contact heat exchanger/sulfuric acid scrubber concept, as discussed in Section 19.2.2, may be required.

The temperature of the HTGR heat source can also have a significant impact on the helium heating pinch temperature, which is the minimum temperature at which heat can be extracted from the secondary helium heat source. From Figure 19.17, the lowest heating target (best efficiency) at the highest temperature (900°C) was obtained at the highest pressure (90 bar), while the lowest heating target at the lowest temperature (700°C) was obtained at the lowest pressure (15 bar). Comparing the helium heating pinch temperatures at these two extremes as a function of feed concentration in Figure 19.18 [98], it can be seen that the lower heat source temperature gives the higher helium heating pinch temperature, greatly narrowing the temperature range over which heat can be efficiently transferred from the HTGR to the bayonet reactor. This is a consequence of the assumption that catalyst activity is insufficient below a certain threshold temperature (here assumed to be 675°C). As a result, the same heat of reaction must be supplied over a narrower temperature range, causing the utility pinch temperature to be determined by the catalyst bed inlet conditions instead of the recuperation pinch point. Therefore, lowering the HTGR operating temperature not only lowers the upper end of the temperature range over which heat can be

transferred from the secondary helium loop to the bayonet reactor, but it may also raise the lower end, greatly reducing the fraction of HTGR heat output that can be applied to sulfuric acid decomposition.

More details are available elsewhere [98].

19.4 *Process Flowsheet*

One of the first complete HyS flowsheets was presented in a conceptual design report prepared by Westinghouse for NASA [2]. The best illustration of this flowsheet appears in Knoche and Funk's second-law analysis [58], and is reproduced in Figure 19.19. The salient features include an HTGR heat source operating at 1010°C, a microporous diaphragm SDE operating at 90°C and 26 bar to produce 75 wt % sulfuric acid, and a sulfuric acid decomposer operating at 871°C and 3.8 bar. SO_2 is separated from O_2 by first compressing the decomposition product to 52 bar (in stages, with intercoolers and condensers to remove liquid water) and then cooling while expanding to 25 bar to achieve -97°C temperature and a relatively clean split between liquid SO_2 and gaseous O_2. The cell potential was assumed to be 450 mV.

The net thermal efficiency of this flowsheet was estimated to be 45% on a higher heating value (HHV) basis, which is equivalent to 38% (LHV basis).[2] This value was confirmed in Knoche and Funk's subsequent analysis.[58] With the over thirty years' perspective from which these results are now viewed, it is clear that some of the underlying assumptions are unrealistically optimistic and should be changed. However, the diminishing effect of these changes has been offset by advances in process integration, particularly pinch technology.

A more recent HyS flowsheet has been presented by SRNL and others [97]. It is based on the use of a PEM-type SDE and a bayonet decomposition reactor. Many earlier efforts to prepare flowsheets for HyS and other thermochemical processes used somewhat simplified and idealized designs. The SRNL-led team, which included experienced industrial partners, attempted to develop a flowsheet reflecting normal industrial practices, including realistic operating conditions, such as heat exchanger approach temperatures, conservative ambient design values, and the need for blow-down and make-up streams. A summary of this flowsheet is presented in the following.

19.4.1 Integrating a PEM SDE with a Bayonet Decomposition Reactor

A PEM-type electrolyzer using a Nafion® membrane was assumed as the basis for the SDE design. Use of Nafion® membranes limits the SDE anolyte product to 50 wt % H_2SO_4 at 100°C and 20 bar. Higher temperatures give better kinetics, but can't be tolerated by Nafion® PEMs. SDEs using advanced, higher temperature membranes are being investigated, and successful implementation of these components may permit an improved flowsheet design using higher temperature SDE operation and more concentrated sulfuric acid anolyte. The pressure was selected to provide product hydrogen under pressure, which minimizes downstream compression requirements. The operating pressure was limited, however, by phase equilibrium considerations. Higher pressures favor SO_2 solubility, but are limited by SO_2 vapor pressure – two liquid phases could otherwise form in the SDE in some circumstances.

Anolyte effluent contains unreacted SO_2 as well as traces of O_2. To integrate the SDE with a high-temperature decomposition reactor, most of the anolyte needs to be recycled. The remaining

product stream, containing one mole of H_2SO_4 for each mole of H_2 produced in the SDE, is passed on. Unreacted SO_2 and trace O_2 first need to be removed from this stream, along with about one-third (to yield 60 wt % H_2SO_4) to three-quarters (to yield 80 wt % H_2SO_4) of the water content. A detailed analysis of the bayonet reactor has shown that a 65-to-80-wt % H_2SO_4 feed concentration gives the best energy utilization [98]. Similarly, the bayonet product has to be cooled, unreacted H_2SO_4 recycled, O_2 removed, and the remaining SO_2 and water condensed and combined with recycled, spent anolyte to form fresh anolyte feed.

The simplest way to remove unreacted SO_2 and trace O_2 from the SDE product is by dropping the pressure. This requires recompressing the predominantly SO_2 and trace O_2 vapor stream that is out-gassed so that it can be recycled to the SDE feed system. The shaft work required is not excessive and the separation can be made without any additional heat input.

A variety of methods are available to concentrate degassed SDE product. All consume energy, some more than others. For example, dropping the pressure of a 50% H_2SO_4 solution at 100°C isothermally, from 20 bar to just under 0.05 bar, can concentrate the liquid residue to 75% H_2SO_4 while consuming 169 kJ/mol H_2SO_4 heat duty. Water boils off in the vapor phase. Heating 50% H_2SO_4 at 20 bar from100°C to 317°C could just as easily boil off the water instead and would need 246 kJ/mol H_2SO_4 heat duty. In either case, excessive heating would be required, causing the sum of the acid concentration and decomposition duties to exceed the 450-kJ/mol H_2 practical upper limit. A recuperative method is clearly needed.

SRNL has chosen vacuum distillation with recuperative preheating/partial vaporization of the feed streams to concentrate the SDE product. Vacuum is maintained using a two-stage steam ejector, keeping temperatures high enough to allow use of cooling water in the condenser, yet low enough to permit metallic materials of construction. Water removed in the concentration process is condensed and recycled to the SDE feed system. The vacuum column bottoms, containing concentrated sulfuric acid at 75 wt % H_2SO_4, can be pumped to the necessary pressure and fed directly to the bayonet reactor.

Effluent from the bayonet reactor is readily separated into unreacted H_2SO_4 feed and SO_2/O_2 product by means of a vapor/liquid split. The acid is simply recycled to the vacuum still. The vapor is cooled further and let down to the pressure of the SDE feed system, resulting in a three-phase mixture: wet liquid SO_2, a saturated solution of SO_2 in H_2O, and wet O_2 gas contaminated with SO_2. The O_2 gas can be scrubbed with the water collected in the concentration process to remove most of the SO_2. The two liquid phases can then be combined with that water and with recycled, spent anolyte to form fresh anolyte feed.

Integration of the PEM SDE and the bayonet reactor as described above results in a flowsheet that uses only proven technology, with the sole exception of the SDE and the decomposition reactor. Thus, the flowsheet itself does not introduce any additional technical hurdles. This should help give the performance projections greater credibility.

19.4.2 The PEM SDE / Bayonet Reactor Hybrid Sulfur Flowsheet

An Aspen Plus flowsheet was prepared according to the integration approach described in the preceding section. The flowsheet is shown in Figure 19.20. Stream data for this flowsheet are tabulated in Table 19.2. The basis is a 1-kmol/sec H_2 production rate.

The flowsheet simulations used OLI Systems, Inc.'s Mixed Solvent Electrolyte (MSE) properties model [124], which has been shown to represent the H_2SO_4-H_2O system very well over its entire composition range and at temperatures as high as 500°C [116]. (The Aspen-OLI interface allows OLI Engine use from within Aspen Plus.) Spot checks of the OLI MSE model's representations of SO_2-H_2O and SO_2-H_2SO_4-H_2O vapor-liquid and liquid-liquid equilibria against the available data showed generally good agreement (e.g. see Figures 19.21 [125-127] and 19.22 [128-130]).

Block EL-01, on the left-hand side of Figure 19.20, is the SDE. Stream 1 is the H_2O feed to the cathode, while stream 2 is the anode feed, containing 15.5 wt % SO_2 dissolved in 43.5 wt % H_2SO_4. Both streams are at 21 bar, and the SDE imposes a frictional pressure drop of 1 bar. The quantity of SO_2 dissolved in stream 2 is just below the saturation point (beyond which a separate liquid SO_2 phase would form) and the target concentration of H_2SO_4 in the anolyte product following the reaction is 50% by weight (excluding SO_2).

A detailed unit operation model of the SDE has yet to be developed, so a "black box" approach was used instead as described below:

- A net flux of H_2O is imposed from cathode to anode (arbitrarily set at 1 kmol H_2O / kmol SO_2 reacted) due to the difference in water activity across the PEM.
- Reaction (19.2) occurs with an assumed SO_2 conversion of 40%.
- All H_2 exits the cathode with the remaining water from stream 1 via stream 3.
- Everything else exits the anode via stream 11.
- The temperatures of streams 3 and 11 are identical and calculated to make the enthalpy change between feed and product streams equal to the electrical work performed with an assumed cell potential of 0.6 V.
- Streams 3 and 11 exit the SDE at a pressure 1 bar lower than streams 1 and 2, respectively.

The temperature of streams 3 and 11 is controlled to 100°C by adjusting the temperature of anolyte feed stream 2 using heat exchanger HX-06. Experimental evidence for the diffusion of water from the cathode to the anode in a PEM SDE has been provided by Staser and co-workers [104] at the University of South Carolina (USC). The assumed flux of 1 kmol H_2O / kmol SO_2 reacted is an estimate consistent with USC data that needs to be refined with further experiments.

The assumed SO_2 conversion of 40% is a design goal based on experimental data from SRNL and USC. Higher conversion means less unconverted SO_2 to recycle, but then cell potential will likely increase due to lower average SO_2 concentration at the anode. Conversions in excess of 20% are routinely achieved in SDE development experiments at SRNL, and over 50% at USC using gaseous SO_2 feed. The trade-off between cell potential and recycle effects will ultimately determine the optimum value of conversion once the relationship between conversion and cell potential has been established.

Stream 3 is cooled by interchange with stream 17 in heat exchanger HX-01, maintaining a 10°C minimum temperature difference. The remaining vapor is removed as stream 5 in knock-out KO-01 and fed to the H_2 Dryer (DR-01), which removes all of the H_2O as stream 8. Pure, dry H_2 product exits as stream 6 at 40°C and 20 bar. H_2O "feedstock" (stream 9) is combined with recycled H_2O (stream 7) and that removed by the dryer (stream 8) and pumped back to the cathode using pump PP-01. Since the flux of water across the PEM from the cathode to the anode due to diffusion was deliberately set at exactly 1 kmol H_2O / kmol SO_2, the water-splitting material balance closes.

The H_2 Dryer was not designed in detail. Regeneration requirements were not taken into account. Simple cooling to 40°C should condense most of the water; the remainder could be absorbed by a molecular sieve. This should not significantly affect energy efficiency.

Anolyte product (stream 11) is split at SP-01, sending enough H_2SO_4 to decomposition via stream 12 to make all of the SO_2 needed for the SDE. The remainder (about 80% of stream 11) is recycled to the anolyte prep tank (TK-01) via stream 48, which is cooled by interchange with stream 17 in heat exchanger HX-05 with a 10°C minimum temperature difference.

The anolyte product pressure is dropped in three stages before entering the Vacuum Column (TO-01). Throttling valve VV-01 drops the pressure to atmospheric, vaporizing over 90% of the SO_2 and all but a trace of the dissolved O_2 for removal in knock-out KO-02 via stream 52, along with some H_2O. The pressure is then dropped to slightly over 0.3 bar via throttling valve VV-02.

A steam ejector (EJ-01) provides the necessary suction. Nearly 90% of the remaining SO_2 and a little more H_2O are vaporized and removed in knock-out KO-03 via stream 69. Pressure is dropped once more to match the feed stage pressure in the Vacuum Column (0.11 bar) by means of throttling valve VV-03. The SO_2–free acid (stream 17) is first heated and partially vaporized by interchange with six other streams in heat exchanger HX-02, maintaining a 10°C minimum temperature difference with all of them, before being fed to the 5th equilibrium stage of TO-01.

The second-stage steam ejector, EJ-02, maintains the Vacuum Column overhead pressure at 0.09 bar. Pressure drop from bottom to top is set at 0.04 bar, placing the bottoms at 0.13 bar. This is feasible with ceramic or metallic structured packing, as can be demonstrated with Aspen Plus RadFrac Pack Sizing calculations. TO-01 has 9 equilibrium stages, including a partial condenser (stage 1) and a kettle reboiler (stage 9). The reflux/distillate ratio is 0.1, with a distillate vapor fraction of 0.001. A bottoms concentration of 75% H_2SO_4 can be achieved by adjusting the distillate rate to just under 4.4 kmol/sec. At these conditions, the bottoms temperature is 122.9°C and the reboiler requires 75.5 kJ/mol H_2 duty, which can be supplied with a low-pressure steam utility. The overhead is at 40°C and requires 210.5 kJ/mol H_2 cooling duty, which can be provided using a conventional cooling water system. (This may not be possible during summertime in some climates, because it would require the cooling water supply temperature not to exceed 30°C. In that case, the column pressure could be increased if necessary.)

Bottoms product from the Vacuum Column (stream 19), containing 75 wt % H_2SO_4 at 122.9°C and 0.13 bar is pumped directly to the Decomposition Reactor (bayonet reactor, RX-01) by means of pump PP-02, which raises the pressure to 86 bar. A separate simulation (detailed in References

[95] and [98]) was used to establish the minimum high-temperature heating target for RX-01, 340.3 kJ/mol H_2, which was set equal to the actual high-temperature heat requirement (with the implicit assumption of perfect recuperation). An HTGR outlet temperature of 950°C was assumed, leading to a peak process temperature of 875°C, as shown in Figure 19.6. At these conditions, fractional conversion of H_2SO_4 was 48.1%, and the effluent temperature was 254.7°C with a vapor fraction of 20.4% (assuming 10°C minimum temperature difference for recuperation).

Bayonet reactor product (stream 21) is separated into its liquid (stream 22) and vapor (stream 31) components by knock-out KO-04. The pressure of the liquid product is then dropped to 21 bar using throttling valve VV-04. This allows about 80% of the dissolved SO_2 and 99% of the dissolved O_2 to be removed in knock-out KO-05. The remaining liquid (stream 24) is a 59.3 wt % H_2SO_4 solution at 233.4°C that can be recycled to the Vacuum Column. The vapor that was removed (stream 47) contains some of the SO_2 and O_2 products of the decomposition reaction. It is sent to the SO_2 Absorber (TO-02) for separation.

Recycled unconverted H_2SO_4 (stream 24) is depressurized in three stages before being fed to the Vacuum Column in a manner identical to the SDE anolyte product. Throttling valves VV-05, VV-06, and VV-07 serve this purpose, and act with knock-outs KO-06 and KO-07 to strip out all but a trace of the dissolved SO_2 and O_2 along with some H_2O via streams 54 and 71. The resulting 67.1 wt % H_2SO_4 stream (number 29) is heated and partially vaporized by interchange with two other streams in heat exchanger HX-03, maintaining a 10°C minimum temperature difference with both. It is then fed to equilibrium stage 8 of the Vacuum Column.

Hot vapor from the bayonet reactor product (stream 31) is cooled to 40°C and partially condensed in three steps (by heat exchangers HX-04A, HX-04B, and HX-04C). It is then separated into one vapor and two liquid phases in knock-out decanter KO-08. The lighter liquid phase consists of H_2O with 27.3 wt % dissolved SO_2 and a small amount of O_2, while the heavier phase is liquid SO_2 containing 3.7 wt % H_2O and a small amount of O_2. HX-04A is cooled by interchange with the recycled acid feed to the Vacuum Column (HX-03), while HX-04B interchanges with the anolyte product feed to the Vacuum Column (HX-02). HX-04C rejects heat to cooling water. In practice, it would not be necessary to separate the two liquid phases in KO-08, since both are ultimately sent to the Anolyte Prep Tank. However, the split is shown to demonstrate that separate aqueous and SO_2 phases can and do exist at these conditions.

The vapor and liquid effluents from KO-08 are let down in pressure from 86 bar to 21 bar via throttling valves VV-08, VV-09, and VV-10, which leads to further phase changes. Vapor is separated from residual liquids in knock-outs KO-09, KO-10, and KO-11, and fed to the bottom of the SO_2 Absorber, while the liquid phases are collected by the Anolyte Prep Tank.

Second-stage ejector (EJ-02) effluent (stream 85) is cooled to 40°C with cooling water in heat exchanger HX-12. The condensate (stream 86) is pumped to waste by pump PP-09 to help ensure that any contaminants that may have entered with the steam (stream 84) are purged from the system. Remaining vapors (stream 89) are sent to knock-out KO-14, which is maintained at 0.3 bar by means of the first-stage ejector, EJ-01. KO-14 also receives partially condensed vapors from knock-outs KO-03 (stream 70) and KO-07 (stream 73); these streams are cooled with cooling

water to 40°C by heat exchangers HX-09 and HX-10B. Some of the heat released by condensing vapor (heat exchanger HX-10A) is transferred by interchange to HX-02. The aqueous phase removed by KO-14 (stream 74) is pumped to the 3rd equilibrium stage of the SO_2 Absorber by pump PP-07.

First-stage ejector (EJ-01) effluent (stream 78) is cooled to 40°C with cooling water in heat exchanger HX-11. This ejector's condensate (stream 79) is also sent to waste. The remaining vapors (stream 80) are sent to knock-out KO-12, which receives partially condensed vapors from knock-outs KO-02 and KO-06 as well. Vapors removed in knock-out KO-02 (stream 52) are first cooled to 40°C with cooling water by heat exchanger HX-07, while those removed in knock-out KO-06 (stream 54) are cooled to 40°C in a series of three heat exchangers: HX-08A, by interchange with HX-03; HX-008B, by interchange with HX-02; and HX-08C, using cooling water.

A dilute solution of SO_2 in H_2O is recovered as liquid in knock-out KO-12 (stream 67). It is pumped to the 5th equilibrium stage of the SO_2 Absorber by pump PP-06. The remaining vapor (stream 58) is a moist SO_2 stream containing about 0.3 mol% O_2. It must be compressed to 21 bar before it can be fed to the bottom of the SO_2 Absorber. The three-stage SO_2 Recycle Compressor, CO-01, is used for this purpose. It has intercoolers and knock-outs that cool the outlet of each stage to 40°C and remove any condensate.

The first stage intercooler and knock-out condense and remove about 5% (by volume) of the feed as a 12.9% (by weight) solution of SO_2 in H_2O (stream 62) at 2.78 bar. Pump PP-04 sends this

stream to the Anolyte Prep Tank. The second stage intercooler condenses most of the remaining vapors, which are removed by the knock-out (stream 64) as nearly pure liquid SO_2 containing 0.8% H_2O by weight and a trace of O_2 at 7.65 bar. Pump PP-05 sends this stream to the Anolyte Prep Tank. Partially condensed effluent from the last stage (stream 59) is fed to knock-out KO-13. Less than 1% (by volume) of the original feed to CO-01 (stream 58) remains in the vapor phase (stream 66) after compression. It is fed to the bottom of the SO_2 Absorber. Slightly more than twice that quantity is removed as condensate (stream 60) and sent to the Anolyte Prep Tank. Stream 66 is roughly 65% O_2/35% SO_2 (by volume), while stream 60 is 99.9% SO_2 (by weight), with minor amounts of O_2 and H_2O.

The SO_2 Absorber has eight equilibrium stages and operates at 21 bar pressure with an assumed negligible pressure drop. Liquid distillate from the Vacuum Column (stream 81, 99.9% H_2O by weight, with 0.1% SO_2 at 40°C) is fed by pump PP-08 to the top stage. Effluent from the second-stage ejector knock-out (stream 75), containing 98.7% H_2O by weight, with 1.3% SO_2 at 41°C is fed to stage 3. The first-stage ejector knock-out effluent (stream 68) is routed to stage 5. It contains 95.2% H_2O by weight, with 4.8% SO_2 at 40°C. Vapor effluents from five knock-outs and the Anolyte Prep Tank vent are fed to the bottom. SO_2 is scrubbed from the vapor phase as it rises up the Absorber, encountering water with progressively less dissolved SO_2. The overhead product (stream 90) is 98.7% O_2 (by volume) at 41°C and 21 bar, with 0.5% H_2O and 0.8% SO_2. It is fed to the O_2 Dryer (DR-02), where the H_2O and SO_2 are removed (stream 93) and routed to the Anolyte Prep Tank, leaving a pure O_2 product (stream 91) at 40°C and 21 bar. The SO_2 Absorber bottoms stream (92) contains 14.1% (by weight) SO_2 in H_2O at 82°C and 21 bar, with traces of O_2 and H_2SO_4. It is sent to the Anolyte Prep Tank.

As was the case with the H_2 Dryer, a detailed design for the O_2 Dryer was not made, and regeneration requirements were not taken into account. Selective absorption of SO_2 and H_2O by a molecular sieve is one possible method. This simplification is likewise not expected to alter the outcome significantly.

All of the SO_2 produced by the decomposition of H_2SO_4, as well as that recovered from the SDE anolyte effluent and any liquids end up in the Anolyte Prep Tank. The resulting liquid (stream 51) is a 43.5% H_2SO_4 solution (by weight), containing 15.5% SO_2 at a temperature of 84.7°C and a pressure of 21 bar. This is fed to the SDE anode after adjusting the temperature in heat exchanger HX-06 (by interchange with stream 17 via HX-02) to achieve a 100°C SDE outlet temperature. The anolyte feed (stream 2) temperature is 78.8°C.

Make-up sulfuric acid is added to the Anolyte Prep Tank as needed to compensate for SO_2 and H_2O losses due to the ejector blow-downs. (More water is wasted via stream 88, which also contains some SO_2, than enters with streams 77 and 84.) The quantity of make-up needed is very small (about 0.008 kmol total/kmol H_2 product) and the sulfur content, at 23.6% H_2SO_4 (by weight), corresponds to only about 0.0004 kmol S/kmol H_2 product.

19.4.3 Flowsheet Energy Requirements

Heat exchanger specifications are presented in Table 19.3. External heat input is required in only two places: the bayonet reactor (RX-01) and the Vacuum Column (TO-01) reboiler. The bayonet reactor receives 340.3 kJ/mol H_2 high-temperature heat from the HTGR. The reboiler, however,

does not need such high temperatures since it operates in the 100 to 125°C range. The amount required, only 75.5 kJ/mol H_2., can be supplied with low-pressure steam. Heat rejection to cooling water adds up to 252.9 kJ/mol H_2, with over 80% attributable to the Vacuum Column condenser. Recuperation takes place in exchangers HX-02 and HX-03, accounting for 130.5 and 31.8 kJ/mol H_2 heat exchange, respectively.

The vacuum ejectors require a small quantity of steam for their operation (streams 77 and 84, 1:1 molar entrainment ratio basis). This corresponds to an equivalent 1.31-kJ/mol H_2 heat duty for the estimated 0.0277-kmol/sec flow of low-pressure steam. At two orders of magnitude smaller than the bayonet reactor duty, it has little effect on the efficiency calculation. Nevertheless, ejector design should be more closely examined to confirm the validity of this simplification.

Electric power requirements are detailed in Table 19.4. The SDE accounts for the majority (115.8 kJ/mol H_2) of the 120.9 kJ/mol H_2 electric energy consumed by the flowsheet. Most of the rest, about 2.8 kJ/mol H_2, is attributable to SO_2 Recycle Compressor. The actual pumping requirement will be somewhat higher because frictional losses due to flow through equipment have been ignored. Assuming a thermal-to-electric conversion efficiency of 33% (BWR/PWR power), the total electric power requirement is equivalent to a heat input of 366.4 kJ/mol H_2. If HTGR power were to be used instead (45% conversion efficiency), the equivalent heat input would be 268.7 kJ/mol H_2.

The total heat consumed by the process is 340.3 + 75.5 + 1.3 = 417.1 kJ/mol H_2, which meets the ≤450 kJ/mol H_2 goal discussed in Section 19.3.3. Adding the thermal equivalent of the power

consumption (assuming a BWR/PWR power source), this flowsheet requires a total of 783.5 kJ/mol H_2 of primary energy, comparing favorably with BWR/PWR-powered water electrolysis at 1080 kJ/mol H_2 [95]. A significant portion of the heat could be supplied by another source. The 76.8-kJ/mol H_2 heat duty of the Vacuum Column reboiler and steam ejectors could be provided by a low-pressure steam utility that recovers low-grade, possibly waste haste from another primary source. In that case, the primary (nuclear) energy (HTGR heat + BWR/PWR power) requirement for this flowsheet would be only 706.7 kJ/mol H_2, making the comparison with direct electrolysis even more favorable.

Using an HTGR power source instead would reduce the primary energy requirement from 783.5 to 685.8 kJ/mol H_2, which still compares favorably with HTGR-powered water electrolysis at 791 kJ/mol H_2 [95]. The differential would be even greater if the Vacuum Column reboiler and steam ejectors could make use of low-grade heat from an alternative source.

19.4.4 Flowsheet Discussion

The HyS flowsheet presented above combines a PEM SDE with a bayonet decomposition reactor and otherwise uses only proven chemical process technology. If the SDE and high-temperature decomposition reactor perform as projected (600-mV cell potential, 40% conversion, 50-wt % H_2SO_4 product; 950°C HTGR operating temperature, 50°C drop between the primary and secondary helium coolants, 25°C minimum temperature difference between helium coolant and process stream, 10°C minimum temperature difference for recuperation, adequate heat transfer characteristics) the flowsheet process will split water into H_2 and O_2 while consuming 340.3 kJ/mol H_2 high-temperature heat, 76.8 kJ/mol H_2 low-temperature heat, and 120.9 kJ/mol H_2

electric power. Should the ultimate source of the electric power be a BWR/PWR (electricity from heat at 33% conversion efficiency), the net thermal efficiency would be 30.9%, LHV basis, excluding the power needed for helium circulators. This is significantly more efficient than alkaline electrolysis coupled with BWR/PWR power (22.4%, LHV basis). A higher net thermal efficiency, 35.3%, LHV basis would be attainable with HTGR power, which is still better than HTGR-powered electrolysis (30.6%, LHV basis).

Recent developments indicate that there may be considerable upside for HyS net thermal efficiency. The results of preliminary experiments with PBI membranes at USC show that significantly higher acid concentrations, in excess of 65% H_2SO_4 by weight may be feasible with PBI PEM SDEs [131]. If this work is successful, the 75.5-kJ/mol H_2 heat duty for the Vacuum Column would be eliminated (recuperative heating would suffice) and the bayonet heat requirement could possibly be lowered to 321 kJ/mol H_2 (80 wt % acid feed). Using HTGR power with an assumed conversion efficiency of 45%, the primary energy requirement would then be only 321 + 1.3 + 120.9/0.45 = 591 kJ/mol H_2. This would give a net thermal efficiency of 40.9%, LHV basis, which is more efficient than the original Westinghouse design. It also compares very favorably with water electrolysis at 30.6%. If the more optimistic estimate of 52% HTGR power conversion efficiency used in some hydrogen production scenarios [120] were to be adopted instead, the net thermal efficiency would increase to 43.6%, LHV basis (51.6%, HHV basis).

The unit cost of H_2 production ($/kg H_2) will ultimately determine whether the HyS process will be commercialized. HyS plants will be the preferred choice for H_2 production using nuclear power only if they can split water into H_2 and O_2 more economically than simple electrolysis or other

competing process.

It should be noted that moving hot, pressurized helium through ductwork and heat exchangers will consume a significant amount of energy, which is not accounted for in Table 19.4. The primary and secondary loop circulators for the HTGR heat source (see Figure 19.6) will require on the order of 20 kJ/mol H_2 electric power; the exact figure depends on the HTGR design details. While the work performed by these circulators is eventually recovered as additional heat, it comes with a conversion loss penalty that should be included in the efficiency calculation.

Finally, some additional work will be needed to reject 252.9 kJ/mol H_2 waste heat to cooling water (i.e. to pump water to and from the cooling tower). However, the amount should be much smaller than that needed for the circulators and should not materially affect the results.

19.5 *Process Engineering*

The process engineering challenges for the HyS cycle are somewhat less than the challenges for either the other thermochemical water-splitting processes or even a high-temperature steam electrolysis (HTSE) plant. HyS has two major chemical reactions, which involve only compounds of hydrogen, oxygen and sulfur. This minimizes material challenges and simplifies separation steps, unit operations and other process engineering requirements. All process streams contain only fluids, and except for the two reaction operations, the chemical processing steps consist mainly of conventional vapor-liquid separations, such as flash evaporation, distillation, and gas/liquid absorption. Since only sulfuric acid and its derivative compounds are recycled between the two main reaction steps, there are no requirements for separating different chemical species

(e.g. sulfur compounds from iodine or bromine compounds, etc.) and the issues of cross-contamination between steps are eliminated. The single gas/gas separation involves the removal of sulfur dioxide from the by-product oxygen stream. However, since the majority of the SO_2 can be removed by condensation under the proper temperature and pressure conditions, the final purification processing of the oxygen is minimized.

The relative simplicity of the HyS cycle, however, does not mean that the process engineering design is not challenging. Processing of sulfuric acid at moderate temperatures is a well-known industrial practice, but processing it under the extreme temperatures and pressures required for the HyS process presents unique challenges with regard to materials of construction and equipment design. Furthermore, portions of the flowsheet involve sulfuric acid containing dissolved sulfur dioxide, which results in additional material corrosion concerns. The process engineering challenges were addressed in a detailed study performed by SNRL and a team of industrial partners [97]. A comprehensive commercial-type flowsheet resulting from this work was presented in the previous section. All major equipment was sized, materials of construction selected, and capital costs estimated.

The two most important pieces of equipment are the SDE and the acid decomposer. The SDE is a modular component by its nature, and a nuclear hydrogen plant requires a large number of SDE units operating in parallel. Each SDE in turn is composed of a stack of electrochemical cells. Many of the SDE equipment design and process engineering issues can be addressed by recognizing the similarities between the requirements for a large SDE module and the electrochemical cells used in commercial chlor-alkali plants. Like the SDE, modern chlor-alkali

cells use a proton-exchange membrane cell design, and they can be built with membranes containing up to 4 m^2 of active cell area. A proposed conceptual design of a HyS SDE is shown in Figure 19.23. It consists of 200 cells connected in series and constrained between steel end plates using tie-rods. The cells consist of circular bipolar plates and an MEA using a PEM electrolyte with 1 m^2 of active area. Gaskets between cells provide sealing for operating pressures up to 20 bar. An alternative approach would be use a stack design with a small nominal differential pressure across the seals by enclosing the entire stack inside a pressure vessel. Such an approach had been suggested by Westinghouse [2].

Based on operation at 500 mA/cm^2 current density and an average cell voltage of 600 mV, the module would produce 38 kg/hr of hydrogen with an energy content of 1.5 MW, HHV basis. The module is approximately 1.22 m (48 inches) in diameter and has an overall length, including end plates and other structural components, of 3.15 m (124 inches). A nuclear hydrogen plant will require multiple modules, including extra modules for capacity margin and to provide for maintenance. A 500-MW_{th} HTGR plant would require approximately 192 SDE modules, containing a total of 38,400 individual cells. This can be contrasted with a similarly sized HTSE plant, which will need over one million high-temperature ceramic cells. The SDE modules might be arranged in four separate cell rooms or buildings, with 48 modules per cell room. A plot plan for a typical cell room is shown in Figure 19.24.

Anolyte and catholyte tanks, pumps and electrical equipment are located near the cell rooms. Sulfuric acid piping will be needed to connect the cell rooms to the acid concentration and feed preparation portions of the HyS plant. The piping system, however, will only convey liquids at

temperatures of approximately 100°C. This is a much simpler process engineering challenge than that faced by HTSE plants, which are required to convey a mixture of hot steam and hydrogen at 800-900°C from a central point to hundreds and perhaps thousands of individual HTSE modules distributed over a large physical area.

Various designs have been proposed for the acid decomposer portion of the HyS plant. The Öztürk and bayonet decomposer designs were discussed previously. An artist's drawing of a potential large-scale bayonet type decomposer is shown in Figure 19.25 [98]. Westinghouse Electric has also proposed a somewhat different recuperative-type decomposition reactor that combines both acid concentration and acid decomposition in a single piece of equipment [62-63]. The Westinghouse design would require two large decomposers for a single 500-MW_{th} HTGR nuclear hydrogen plant.

As mentioned previously, the balance of the process design, with the exception of the SDE and acid decomposer, utilizes mostly conventional process equipment, although the material issues can be unique. It should be recognized that system integration resulting in an efficient process design is critical to obtaining a high overall HyS process efficiency. For example, the sulfuric acid product leaving the SDE section must be concentrated prior to its introduction into the acid decomposition section. The efficient use of heat recuperation and an optimized design based on pinch analysis can help to minimize the additional energy needed for this step. Furthermore, any increase in acid concentration exiting the SDE will minimize the amount of water that needs to be evaporated in the acid concentration step, thus reducing energy demand. The use of advanced, high temperature membranes in the SDE is one means of permitting electrolysis operation with

higher acid concentration.

The conceptual design reported in Reference [97] used traditional engineering procedures to size all the major process equipment of the HyS plant, aiming at the best possible design from an economic point of view. Major equipment lists were prepared showing equipment type, physical size, mechanical design conditions and materials of construction. Shell-and-tube heat exchangers were selected in most cases as heat transfer devices. They were sized in detail, following standard TEMA classification, rules and suggestions and varying the most important parameters and degrees of freedom (e.g. tube diameters, tube length, baffle typology and arrangement, etc.) to get to the best solution. Knock-out pots, flash drums, etc were sized adopting traditional methodologies choosing vertical or horizontal equipment depending on the specific working conditions. Pumping equipment (centrifugal pumps, rotary pumps, and diaphragm pumps) was selected and sized to provide the most suitable pump models accounting for flow rates and pressure head to be supplied. A three-stage centrifugal compressor was adopted to recycle SO_2 in the acid decomposition section, internally recovering (in the H_2SO_4 section) the heat available from the inter-cooling process. The vacuum H_2SO_4 concentration column and the SO_2 absorber were sized as packed towers considering traditional sizing methods.

The selection of materials of construction for the equipment represents a fundamental aspect of the plant design, which can lead to wide variations of the total capital cost of the HyS plant. All the components (with the exception of the SDE and the acid decomposition reactor) were sized considering only well-known, traditional metal materials capable of resisting the actual working conditions. In the case of the product purification section of the plant, almost all of the equipment

is made of carbon steel (CS) material. Likewise, components of the feed and utility supply section, which are in contact with water, are assumed to be made of CS material.

As for the other parts of the plant, where sulfur compounds and hydrogen (and water) circulate, various corrosion-resistant materials were selected. In some cases commercial experience with conventional sulfuric acid plant operation may lead to somewhat different selections than those used in the SRNL study, and this should be investigated. However, as cautioned previously, the presence of dissolved SO_2 in the sulfuric acid for some streams and the need to operate at higher temperatures and pressures than conventional sulfuric acid plants, introduce additional materials of construction concerns. Therefore, 316L Stainless Steel (SS) was adopted as the baseline material, due to its capability to resist aggressive conditions, such as contact with H_2SO_4 over wide concentration ranges. To resist more difficult environments (in terms of concentrations and operating temperatures) which would attack 316L SS type materials, Carpenter 20-Cb3 and, where appropriate, Hastelloy B3 were adopted. Carpenter 20-Cb3 is an austenitic SS with good resistance to concentrated H_2SO_4 at high temperatures. Hastelloy B3 is a nickel-based alloy which shows good resistance to H_2SO_4 mixtures over a broad range of temperatures and concentrations, with high thermal stability and resistance to pitting corrosion and stress corrosion. 20-Cb3 and Alloy B3 materials were adopted inside the H_2SO_4 section for the most aggressive environments.

The sulfuric acid concentration process equipment is made of 20-Cb3 and Alloy B3 materials. In particular, the shell of the H_2SO_4 Vacuum Column (with ceramic packing internals) has been assumed to be made of CS material, with Hastelloy B3 internal cladding. The two concentration flashes are made of 20-Cb3 and Alloy B3 (for higher temperatures and concentrations) and the

H_2SO_4 decomposer feed pump has been assumed to be made of Alloy B3. Likewise, the two flashes, operating at temperatures of 255 ºC (528 K) and 234 ºC (507 K) respectively, which separate unreacted H_2SO_4 from the other compounds (SO_2, H_2O and O_2) exiting the bayonet reactor, are made of Hastelloy B3. The remainder of the equipment (i.e. SO_2 separation, SO_2 recirculation, etc.) has been assumed to be made of 316L SS. Particularly aggressive conditions exist in the balance of the electrolysis section equipment, which led to the adoption of 20-Cb3 and Hastelloy B3 as the materials of construction for both heat exchangers and recirculation pumps.

19.6 *Future Technical Challenges*

The current status of the research and development for the HyS thermochemical process has been reviewed, and a process flowsheet and conceptual design for a full-size commercial HyS plant has been discussed. The future technical challenges include the following:

- SDE development: (1) reduction in cell potential through the use of higher temperature operation and improved electrocatalyst; (2) high-temperature membranes with low SO_2 crossover; (3) operation with higher H_2SO_4 product; (4) demonstration of long-time stable operation with minimal operating potential degradation; (5) scale-up to larger cell sizes and multi-cell modules.
- Acid Decomposer: (1) demonstration of a long-life catalyst; (2) operation with convective-heating using a helium heat source; (3) decomposer design and material selections; (4) SiC joining; (5) catalyst replacements methods.
- HyS Process and System Development: (1) integrated system demonstrations at increasingly larger scale; (2) materials of construction validation; (3) capital cost reduction and evaluations.

The majority of the work presented here was the result of activities by the SRNL and its partners, which was part of the US DOE-NE's NHI program. Increasingly, other entities have begun to perform research on the HyS cycle, and international collaboration has increased. A HyS work package has been added to the research subjects under the framework of Very-High Temperature Reactor (VHTR) system in the Generation IV International Forum. These activities are expected to address the remaining technical challenges for the HyS cycle, and to lead to pilot-plant facilities and demonstration of a commercial-scale plant.

References

1. Brecher, L. E., and Wu, C. K. "Electrolytic decomposition of water." US Patent 3,888,750: Westinghouse Electric Corp., June 10, 1975.

2. Farbman, G. H. "Conceptual design of an integrated nuclear hydrogen production plant using the sulfur cycle water decomposition system." Westinghouse Electric Corp., Astronuclear Lab., NASA Contractor Report, NASA-CR-134976, April 1, 1976.

3. Farbman, G. H., Krasicki, B. R., Hardman, C. C., Lin, S. S., and Parker, G. H. "Economic comparison of hydrogen production using sulfuric acid electrolysis and sulfur cycle water decomposition. Final report." Westinghouse Electric Corp., Advanced Energy Systems Division., Electric Power Research Institute Report No. EPRI-EM-789, June 1978.

4. Lu, W. T. P., Ammon, R. L., and Parker, G. H. "A study on the electrolysis of sulfur dioxide and water for the sulfur cycle hydrogen production process." Westinghouse Electric Corp., Advanced Energy Systems Division, NASA Contractor Report, NASA-CR-163517, July 1980.

5. Parker, G. H. "Solar thermal hydrogen production process: final report, January 1978-December 1982." Westinghouse Electric Corp., Advanced Energy Systems Division., US Department of Energy Report DOE/ET/20608-1, January 21, 1983.

6. Brecher, L. E., Spewock, S., and Warde, C. J. "The Westinghouse sulfur cycle for the thermochemical decomposition of water," *Proceedings, 1st World Hydrogen Energy Conference, Miami Beach, FL, USA, March 1-3, 1976* Vol. 1, pp. 9A, 1-16.

7. Carty, R., Cox, K., Funk, J., Soliman, M., Conger, W., Brecher, L., and Spewock, S. "Process sensitivity studies of the Westinghouse sulfur cycle for hydrogen generation," *Proceedings, 1st World Hydrogen Energy Conference, Miami Beach, FL, USA, March 1-3, 1976* Vol. 1, pp. 9A, 17-28.

8. Farbman, G. H., and Brecher, L. E. "Hydrogen production by water decomposition using a combined electrolytic-thermochemical cycle," *Proceedings, 1st World Hydrogen Energy Conference, Miami Beach, FL, USA, March 1-3, 1976* Vol. 1, pp. 9A, 29-50.

9. Spewock, S., Brecher, L. E., and Talko, F. "The thermal catalytic decomposition of sulfur trioxide to sulfur dioxide and oxygen," *Proceedings, 1st World Hydrogen Energy Conference, Miami Beach, FL, USA, March 1-3, 1976* Vol. 1, pp. 9A, 53-68.

10. Parker, G. H., Brecher, L. E., and Farbman, G. H. "Nuclear driven water decomposition plant for hydrogen production " *Proceedings, 11th Conference on Intersociety Energy Conversion Engineering, State Line, NV, USA, September 12-17, 1976* Vol. 2, pp. 1095-1101.

11. Farbman, G. H. "Sulfur cycle water decomposition system," *Proceedings of the ERDA contractors' review meeting on chemical energy storage and hydrogen energy systems, Airlie House, VA, USA, November 8-9, 1976*, pp. 123-128.

12. Farbman, G. H., Ammon, R. L., Hardman, C. C., and Spewock, S. "Development progress on the sulfur cycle water decomposition system," *Proceedings of the 12th Intersociety Energy Conversion Engineering Conference, Washington, DC, USA, August 28-September 2, 1977* Vol. 1, pp. 928-932.

13. Farbman, G. H. "The sulfur cycle water decomposition system," *Proceedings of the DOE Chemical/Hydrogen Energy Systems Contractor Review, Hunt Valley, MD, USA, November 16-17, 1977*, pp. 63-70.

14. Farbman, G. H. "Hydrogen production with the sulfur cycle water decomposition system," *Proceedings of Condensed Papers, Miami International Conference on Alternative Energy Sources, Miami Beach, FL, USA, December 5-7, 1977*, pp. 529-531.

15. Farbman, G. H. "The Westinghouse sulfur cycle hydrogen production process," *Symposium Papers: Hydrogen for Energy Distribution, Chicago, IL, USA, July 24-28, 1978*, pp. 317-337.

16. Farbman, G. H. "The Westinghouse sulfur cycle hydrogen production process: program status," *Hydrogen Energy System: Proceedings of the Second World Hydrogen Energy Conference, Zurich, Switzerland, August 21-24, 1978* Vol. 5, pp. 2485-2504.

17. Ammon, R. L., Parker, G. H., and Farbman, G. H. "Materials considerations for the Westinghouse sulfur cycle hydrogen production process," *Proceedings: Reliability of Materials for Solar Energy Workshop, Denver, CO, USA, December 18, 1978, Vol. 2, Part 2*, pp. 371-394.

18. Farbman, G. H., and Parker, G. H. "The sulfur-cycle hydrogen production process," *Hydrogen: Production and marketing; Proceedings of the Symposium, Honolulu, Hawaii, USA, April 2-6, 1979*. American Chemical Society, ACS Symposium Series, No. 116, 1980, pp. 359-389.

19. Parker, G. H., and Lu, P. W. T. "Laboratory model and electrolyzer development for the sulfur cycle hydrogen production process," *Proceedings of the 14th Intersociety Energy Conversion Engineering Conference, Boston, MA., USA, August 5-10, 1979* Vol. 1, pp. 752-755.

20. Lu, P. W. T., and Ammon, R. L. "Development status of electrolysis technology for the sulfur cycle hydrogen production process," *Hydrogen Energy Progress III: Proceedings of the 3rd World Hydrogen Energy Conference, Tokyo, Japan, June 23-26, 1980* Vol. 1, pp. 439-461.

21. Irwin, H. A., and Ammon, R. L. "Status of materials evaluation for sulfuric acid vaporization and decomposition applications," *Hydrogen Energy Progress III: Proceedings of the 3rd World Hydrogen Energy Conference, Tokyo, Japan, June 23-26, 1980* Vol. 4, pp. 1977-1999.

22. Summers, W. A., Ammon, R. L., and Parker, G. H. "Recent progress on the sulfur cycle hybrid hydrogen production process," *Proceedings of the 15th Intersociety Energy Conversion Engineering Conference, Seattle, WA., USA, August 18-22, 1980* Vol. 3, pp. 2008-2014.

23. Lu, P. W. T. "Technological aspects of sulfur dioxide depolarized electrolysis for hydrogen production," *Hydrogen Energy Progress IV: Proceedings of the 4th World Hydrogen Energy Conference, Pasadena, CA, USA, June 13-17, 1982* Vol. 1, pp. 203-214.

24. Lin, S. S., and Flaherty, R. "Design studies of the sulfur trioxide decomposition reactor for the sulfur cycle hydrogen production process," *Hydrogen Energy Progress IV: Proceedings of the 4th World Hydrogen Energy Conference, Pasadena, CA, USA, June 13-17, 1982* Vol. 2, pp. 599-610.

25. Ammon, R. L. "Status of materials evaluation for sulfuric acid vaporization and decomposition applications," *Hydrogen Energy Progress IV: Proceedings of the 4th World Hydrogen Energy Conference, Pasadena, CA, USA, June 13-17, 1982* Vol. 2, pp. 623-644.

26. Pierre, J. F., and Ammon, R. L. "The Westinghouse sulfur cycle: sulfur trioxide reduction catalyst screening test program," *Hydrogen Energy Progress IV: Proceedings of the 4th World Hydrogen Energy Conference, Pasadena, CA, USA, June 13-17, 1982* Vol. 2, pp. 703-712.

27. Lin, S. S., Parker, G. H., and Stella, M. E. "Solar hydrogen system design considerations," *Proceedings of the 16th Intersociety Energy Conversion Engineering Conference, Atlanta, GA, USA, August 9-14, 1981* Vol. 2, pp. 1430-1435.

28. Brecher, L. E., Spewock, S., and Warde, C. J. "The Westinghouse sulfur cycle for the thermochemical decomposition of water," *International Journal of Hydrogen Energy* **2**(1), 7-15 (1977).

29. Carty, R., Cox, K., Funk, J., Soliman, M., Conger, W., Brecher, L., and Spewock, S. "Process sensitivity studies of the Westinghouse sulfur cycle for hydrogen generation," *International Journal of Hydrogen Energy* **2**(1), 17-22 (1977).

30. Farbman, G. H. "Hydrogen production by the Westinghouse sulfur cycle process: program status," *International Journal of Hydrogen Energy* **4**(2), 111-122 (1979).

31. Lu, P. W. T., Garcia, E. R., and Ammon, R. L. "Recent developments in the technology of sulfur dioxide depolarized electrolysis," *Journal of Applied Electrochemistry* **11**(3), 347-355 (1981).

32. Lu, P. W. T., and Ammon, R. L. "Sulfur dioxide depolarized electrolysis for hydrogen production: development status," *International Journal of Hydrogen Energy* **7**(7), 563-575 (1982).

33. Lin, S. S., and Flaherty, R. "Design studies of the sulfur trioxide decomposition reactor for the sulfur cycle hydrogen production process," *International Journal of Hydrogen Energy* **8**(8), 589-596 (1983).

34. Lu, P. W. T. "Technological aspects of sulfur dioxide depolarized electrolysis for hydrogen production," *International Journal of Hydrogen Energy* **8**(10), 773-781 (1983).

35. Yannopoulos, L. N., and Pierre, J. F. "Hydrogen production process: High temperature-stable catalysts for the conversion of SO_3 to SO_2," *International Journal of Hydrogen Energy* **9**(5), 383-390 (1984).

36. Lu, W. T. P., and Ammon, R. L. "Carbon cloth-supported electrode." US Patent 4,349,428: US Department of Energy, September 14, 1982.

37. Lu, W. T. P. "System using sulfur dioxide as an anode depolarizer in a solid oxide electrolyte electrolysis cell for hydrogen production from steam." US Patent 4,412,895: Westinghouse Electric Corp., November 1, 1983.

38. Beghi, G. E. "A decade of research on thermochemical hydrogen at the Joint Research Centre, Ispra," *International Journal of Hydrogen Energy* **11**(12), 761-771 (1986).

39. Struck, B. D., Junginger, R., Boltersdorf, D., and Gehrmann, J. "Problems concerning the electrochemical step of the sulfuric acid hybrid cycle," *Proceedings, Seminar on hydrogen as an energy vector: its production, use and transportation, Brussels, Belgium, October 3-4, 1978*, pp. 109-123.

40. Struck, B. D., Junginger, R., Boltersdorf, D., Dujka, B., Neumeister, H., and Triefenbach, D. "Development of an electrolytic cell for the anodic oxidation of sulfur dioxide and the cathodic production of hydrogen within the sulfuric acid hybrid thermochemical cycle," *Hydrogen As an Energy Vector: Proceedings of the International Seminar Held in Brussels, Belgium, February 12-14, 1980*. pp. 80-100.

41. Struck, B. D., Junginger, R., Boltersdorf, D., Dujka, B., Neumeister, H., and Triefenbach, D. "Development of an electrolytic cell for the anodic oxidation of sulfur dioxide and the cathodic production of hydrogen within the sulfuric acid hybrid cycle." KFA Juelich, Juelich, Federal Republic of Germany, Report No. EUR-6961, 1980.

42. Struck, B. D., Junginger, R., Boltersdorf, D., and Gehrmann, J. "The anodic oxidation of sulfur dioxide in the sulfuric acid hybrid cycle," *International Journal of Hydrogen Energy* **5**(5), 487-497 (1980).

43. Struck, B. D., Neumeister, H., Dujka, B., and Siebert, U. "Electrolytic cell for the sulfuric acid hybrid cycle," *Hydrogen Energy Progress IV: Proceedings of the 4th World Hydrogen Energy Conference, Pasadena, CA, USA, June 13-17, 1982* Vol. 2, pp. 483-492.

44. Junginger, R., and Struck, B. D. "Separators for electrolytic cells of the sulfuric acid hybrid cycle," *International Journal of Hydrogen Energy* **7**(4), 331-340 (1982).

45. Struck, B. D., Neumeister, H., Dujka, B., Siebert, U., and Triefenbach, D. "Development and scaling up of an electrolytic cell for the anodic oxidation of sulfur dioxide and cathodic production of hydrogen for the sulfuric acid hybrid cycle," in *Hydrogen As an Energy Carrier*. Imarisio, G. and Strub, A. S., eds. Hingham, MA, USA: Kluwer Academic Publishers, 1983, pp. 35-45.

46. Struck, B. D., Neumeister, H., Dujka, B., Siebert, U., and Triefenbach, D. "Development of an electrolytic cell for the anodic oxidation of sulfur dioxide and cathodic production of hydrogen for the sulfuric acid hybrid cycle." Commission of the European Communities, Luxembourg, Report No. EUR-8300EN, 1983.

47. Struck, B. D., Neumeister, H., and Naoumidis, A. "Electrolytic cell for the thermochemical-electrochemical sulfur hybrid cycle for water splitting," *Hydrogen Energy Progress VI: Proceedings of the 6th World Hydrogen Energy Conference, Vienna, Austria, July 20-24, 1986* Vol. 2, pp. 739-743.

48. Takehara, Z., Nogami, M., and Shimizu, Y. "New electrolytic process in hybrid sulfur cycle for hydrogen production from water," *International Journal of Hydrogen Energy* **14**(4), 233-239 (1989).

49. Merkulova, N. D., Boikova, G. V., Zhutaeva, G. V., Tarasevich, M. R., and Shumilova, N. A. "Selectivity of tungsten carbide and platinum in cathodic reactions of the sulfuric acid cycle," *Zhurnal Prikladnoi Khimii (Leningrad)* **57**(10), 2264-2268 (1984).

50. Gorbachev, A. K. "Corrosion resistance of electrode graphites during anodic polarization in sulfuric acid solutions," *Zashchita Metallov* **20**(3), 436-438 (1984).

51. Schepers, H. "Thermodynamic analysis of the sulfur cycle water splitting process," dissertation, Fakultät für Maschinenwesen, Technische Hochschule, Aachen, Germany, 1983.

52. Onstott, E. I. "Measurement of reversible and irreversible energy requirements for hydrogen production in hybrid cycles," *Hydrogen Energy Progress IV: Proceedings of the 4th World Hydrogen Energy Conference, Pasadena, CA, USA, June 13-17, 1982* Vol. 1, pp. 159-165.

53. Appleby, A. J., and Pinchon, B. "Electrochemical aspects of the H_2SO_4-SO_2 thermoelectrochemical cycle for hydrogen production," *International Journal of Hydrogen Energy* **5**(3), 253-267 (1980).

54. Sedlak, J. M., Russell, J. H., LaConti, A. B., Gupta, D. K., Austin, J. F., and Nugent, J. S. "Hydrogen production using solid-polymer-electrolyte technology for water electrolysis and hybrid sulfur cycle." General Electric Co., Electric Power Research Institute Report No. EPRI-EM-1185, September 1, 1979.

55. Feuillade, G., and Caradec, J. Y. "Study of sulfur dioxide electrocatalytic oxidation during the sulfur cycle." Compagnie générale d'électricité, Marcoussis, France, Commission of the European Communities, Luxembourg, Report No. EUR 6603, 1979.

56. Appleby, A. J., and Pichon, B. "The mechanism of the electrochemical oxidation of sulfur dioxide in sulfuric acid solutions," *Journal of Electroanalytical Chemistry* **95**(1), 59-71 (1979).

57. Appleby, A. J., and Pichon, B. "Electrochemical aspects of the sulfuric acid-sulfur dioxide thermoelectrochemical cycle for hydrogen production," *Hydrogen Energy System: Proceedings of the Second World Hydrogen Energy Conference, Zurich, Switzerland, August 21-24, 1978* Vol. 2, pp. 687-707.

58. Knoche, K. F., and Funk, J. E. "Entropy production, efficiency, and economics in the thermochemical generation of synthetic fuels: I. The hybrid sulfuric acid process," *International Journal of Hydrogen Energy* **2**(4), 377-385 (1977).

59. Brown, L. C., Funk, J. F., and Showalter, S. K. "Initial screening of thermochemical water-splitting cycles for high efficiency generation of hydrogen fuels using nuclear power." General Atomics, Report No. GA–A23373, April 2000.

60. Matzie, R., Lahoda, E. J., and Botma, A. "Interfacing the Westinghouse sulfur cycle with the PBMR for the production of hydrogen," *Conference Proceedings, AIChE Spring National Meeting, New Orleans, LA, USA, April 25-29, 2004*, pp. 1034-1043.

61. McLaughlin, D. F., Paletta, S. A., Lahoda, E. J., and Kriel, W. "Revised capital and operating HyS hydrogen production costs," *Proceedings of the 2006 International Congress on Advances in Nuclear Power Plants, Embedded Topical Meeting, Reno, NV, USA, June 4-8, 2006*, pp. 2263-2269.

62. Connolly, S. M., Lahoda, E. J., and McLaughlin, D. F. "Design of recuperative sulfuric acid decomposition reactor for hydrogen generation processes," *Conference Proceedings, AIChE Annual Meeting, Philadelphia, PA, USA, November 16-21, 2008*, pp. 88/1-88/16.

63. Connolly, S. M., Zabolotny, E., McLaughlin, D. F., and Lahoda, E. J. "Design of a composite sulfuric acid decomposition reactor, concentrator, and preheater for hydrogen generation processes," *International Journal of Hydrogen Energy* **34**(9), 4074-4087 (2009).

64. Lahoda, E. J., and McLaughlin, D. F. "Hydrogen generation process with dual pressure multi stage electrolysis." Patent Application, Europe, No. 2008-12190: Westinghouse Electric Company LLC, USA, July 5, 2008.

65. Sink, C. J. "An overview of the U.S. Department of Energy's research and development program on hydrogen production using nuclear energy," *Presentation, AIChE Spring National Meeting, Orlando, FL, United States, April 23-27, 2006*, http://www.aiche-ned.org/conferences/aiche2006spring/session_51/AICHE2006spring-51b-Sink.pdf (accessed October 14, 2009).

66. "Hydrogen posture plan: an integrated research, development and demonstration plan." United States Department of Energy, United States Department of Transportation, December 2006, http://www.hydrogen.energy.gov/pdfs/hydrogen_posture_plan_dec06.pdf (accessed October 14, 2009).

67. Le Duigou, A., Borgard, J.-M., Larousse, B., Doizi, D., Allen, R., Ewan, B. C., Priestman, G. H., Elder, R., Devonshire, R., Ramos, V., Cerri, G., Salvini, C., Giovannelli, A., De Maria, G., Corgnale, C., Brutti, S., Roeb, M., Noglik, A., Rietbrock, P.-M., Mohr, S., De Oliveira, L., Monnerie, N., Schmitz, M., Sattler, C., Martinez, A. O., Manzano, D. d. L., Cedillo Rojas, J., Dechelotte, S., and Baudouin, O. "HYTHEC: An EC funded search for a long term massive hydrogen production route using solar and nuclear technologies," *International Journal of Hydrogen Energy* **32**(10-11), 1516-1529 (2007).

68. Feraud, J. P., Jomard, F., Ode, D., Duhamet, J., Dehaudt, P., Morandini, J., Couvat, Y. D., and Caire, J. P. "Modeling a filter press electrolyzer by using two coupled codes within nuclear Gen. IV hydrogen production," *Proceedings, Global 2007: Advanced Nuclear Fuel Cycles and Systems, Boise, ID, USA, September 9-13, 2007*, pp. 837-844.

69. Jomard, F., Feraud, J. P., Morandini, J., Du Terrail Couvat, Y., and Caire, J. P. "Hydrogen filter press electrolyser modelled by coupling Fluent and Flux Expert codes," *Journal of Applied Electrochemistry* **38**(3), 297-308 (2008).

70. Jomard, F., Feraud, J. P., and Caire, J. P. "Numerical modeling for preliminary design of the hydrogen production electrolyzer in the Westinghouse hybrid cycle," *International Journal of Hydrogen Energy* **33**(4), 1142-1152 (2008).

71. Charton, S., Rivalier, P., Ode, D., Morandini, J., and Caire, J. P. "Hydrogen production by the Westinghouse cycle: modelling and optimization of the two-phase electrolysis cell," *WIT Transactions on Engineering Sciences* **65**(Electrochemical Process Simulation III), 11-22 (2009).

72. Lee, S.-K., Kim, C.-H., Cho, W.-C., Kang, K.-S., Park, C.-S., and Bae, K.-K. "The effect of Pt loading amount on SO_2 oxidation reaction in an SO_2-depolarized electrolyzer used in the hybrid sulfur (HyS) process," *International Journal of Hydrogen Energy* **34**(11), 4701-4707 (2009).

73. Kim, N., and Kim, D. "SO_2 permeability and proton conductivity of sPEEK membranes for SO2-depolarized electrolyzer," *International Journal of Hydrogen Energy* **34**(19), 7919-7926 (2009).

74. Nakagiri, T., Hoshiya, T., and Aoto, K. "Investigation on a new hydrogen production process for FBR," *Proceedings, 2nd Information Exchange Meeting, Nuclear Production of Hydrogen, Argonne, IL, USA, October 2-3, 2003*, pp. 131-143.

75. Nakagiri, T., Ohtaki, A., Hoshiya, T., and Aoto, K. "A new thermochemical and electrolytic hybrid hydrogen production process for FBR," *Nihon Genshiryoku Gakkai Wabun Ronbunshu* **3**(1), 88-94 (2004).

76. Kawamura, H., Mori, M., and Uotani, M. "Basic study of application of electronic conductive ceramic anode to sulfur-based hybrid hydrogen production," *Suiso Enerugi Shisutemu* **30**(1), 42-48 (2005).

77. Kawamura, H., Mori, M., and Uotani, M. "Electron-conductive ceramic powders, cubic titanium-oxide pyrochlore sintered bodies, and electrolysis vessels for sulphur-cycle hybrid hydrogen manufacture." Japan Patent 2005330133: Central Research Institute of Electric Power Industry, Japan, December 2, 2005.

78. Kawamura, H., Chu, S.-Z., Mori, M., and Uotani, M. "Electrochemical properties of ceramic electrodes for sulfur-based hybrid cycle -development of Pd-coated electronic conductive ceramics," *Suiso Enerugi Shisutemu* **31**(2), 32-41 (2006).

79. Nakagiri, T., Kase, T., Kato, S., and Aoto, K. "Development of a new thermochemical and electrolytic hybrid hydrogen production system for sodium cooled FBR," *JSME International Journal, Series B: Fluids and Thermal Engineering* **49**(2), 302-308 (2006).

80. Kawamura, H., Mori, M., and Uotani, M. "Hydrogen preparation using sulfur cycle hybrid method," *Electrochemistry (Tokyo, Japan)* **75**(3), 289-293 (2007).

81. Nakagiri, T., Yamaki, T., Asano, M., and Tsutsumi, Y. "Development of water electrolysis cell for hydrogen production utilizing sulfur dioxide," *Nihon Genshiryoku Gakkai Wabun Ronbunshu* **7**(1), 58-65 (2008).

82. Shimomiya, O. "Apparatus for production of hydrogen by sulfuric acid hybrid process." Japan Patent 2008223098: Ishikawajima-Harima Heavy Industries Co., Ltd., Japan, September 25, 2008.

83. Gorensek, M. B., Buckner, M. R., Summers, W., and Qureshi, Z. H. "Conceptual design for a hybrid sulfur thermochemical process plant," *Conference Proceedings, AIChE Spring National Meeting, Atlanta, GA, USA, April 10-14, 2005*, p. 76F/1.

84. Summers, W. A., and Buckner, M. R. "Hybrid sulfur thermochemical process

development," *DOE Hydrogen Program FY 2005 Progress Report*. May 23, 2005. http://www.hydrogen.energy.gov/pdfs/progress05/iv_g_7_summers.pdf (accessed October 21, 2009).

85. Steimke, J., and Steeper, T. "Generation of hydrogen using electrolyzers with sulfur dioxide depolarized anodes," *Conference Proceedings, AIChE Annual Meeting, Cincinnati, OH, USA, October 30-November 4, 2005*, pp. 581d/1-581d/19.

86. Eargle, J. A., Gorensek, M. B., and Knight, T. W. "Optimization of the thermal efficiency of a hybrid sulfur thermochemical hydrogen process," *Transactions of the American Nuclear Society* **93**(1), 917-918 (2005).

87. Colon-Mercado, H., Ekechukwu, A., and Hobbs, D. "Electrolyzer component testing for hybrid sulfur process," *Abstracts, 58th Southeast Regional Meeting of the American Chemical Society, Augusta, GA, USA, November 1-4, 2006*, p. SRM06-235.

88. Steimke, J., and Steeper, T. J. "Generation of hydrogen using hybrid sulfur process electrolyzer," *Abstracts, 58th Southeast Regional Meeting of the American Chemical Society, Augusta, GA, USA, November 1-4, 2006*, p. SRM06-231.

89. Steimke, J. L., and Steeper, T. J. "Generation of hydrogen using electrolyzer with sulfur dioxide depolarized anode," *Conference Proceedings, AIChE Annual Meeting, San Francisco, CA, USA, November 12-17, 2006*, pp. 126c/1-126c/10.

90. Summers, W. A., and Gorensek, M. B. "Nuclear hydrogen production based on the hybrid sulfur thermochemical process," *Proceedings of the 2006 International Congress on Advances in Nuclear Power Plants, Embedded Topical Meeting, Reno, NV, USA, June 4-8, 2006*, pp. 2254-2256.

91. Colon-Mercado, H. R., and Hobbs, D. T. "Catalyst evaluation for a sulfur dioxide-depolarized electrolyzer," *Electrochemistry Communications* **9**(11), 2649-2653 (2007).

92. Summers, W. A. "Hybrid sulfur thermochemical process development," *DOE 2008 Hydrogen Program Annual Merit Review, Arlington, VA, United States, June 9-13, 2008*. http://www.hydrogen.energy.gov/pdfs/review08/pd_26_summers.pdf (accessed October 21, 2009).

93. Hobbs, D. "Challenges and progress in the development of a sulfur dioxide-depolarized electrolyzer for efficient hydrogen production," *Pittcon Conference & Expo 2009*. Chicago, IL, USA, 2009.

94. Steimke, J. L., Steeper, T., and Herman, D. "Results from testing hybrid sulfur single-cell and three-cell stack," *Hybrid Sulfur Electrolyzer Workshop and Information Exchange, Aiken, SC, United States, April 20-21, 2009*. http://srnl.doe.gov/hse_workshop/Steimke%20Electrolyzer%20Performance.pdf (accessed October 21, 2009).

95. Gorensek, M. B., and Summers, W. A. "Hybrid sulfur flowsheets using PEM electrolysis and a bayonet decomposition reactor," *International Journal of Hydrogen Energy* **34**(9), 4097-4114 (2009).

96. Summers, W. A. "Hybrid sulfur thermochemical cycle," *2009 DOE Hydrogen Program and Vehicle Technologies Program Annual Merit Review and Peer Evaluation Meeting, Arlington, VA, United States, May 18–22, 2009*. http://www.hydrogen.energy.gov/pdfs/review09/pd_13_summers.pdf (accessed October 21, 2009).

97. Gorensek, M. B., Summers, W. A., Bolthrunis, C. O., Lahoda, E. J., Allen, D. T., and Greyvenstein, R. "Hybrid sulfur process reference design and cost analysis." Savannah River National Laboratory, Report No. SRNL-L1200-2008-00002, June 12, 2009 (doi: 10.2172/956960).

98. Gorensek, M. B., and Edwards, T. B. "Energy efficiency limits for a recuperative bayonet sulfuric acid decomposition reactor for sulfur cycle thermochemical hydrogen production," *Industrial & Engineering Chemistry Research* **48**(15), 7232-7245 (2009).

99. Gorensek, M. B., Staser, J. A., Stanford, T. G., and Weidner, J. W. "A thermodynamic analysis of the SO_2/H_2SO_4 system in SO_2-depolarized electrolysis," *International Journal of Hydrogen Energy* **34**(15), 6089-6095 (2009).

100. Hobbs, D. T., Summers, W. A., Colon-Mercado, H. R., Elvington, M. C., Steimke, J. L., Steeper, T. J., Herman, D. T., and Gorensek, M. B. "Recent advances in the development of the hybrid sulfur process for hydrogen production," *Abstracts of Papers, 238th ACS National Meeting, Washington, DC, USA, August 16-20, 2009*, p. NUCL-160.

101. Colón-Mercado, H. R., Elvington, M. C., and Hobbs, D. T. "Component development needs for the hybrid sulfur electrolyzer." Savannah River National Laboratory, Report No. WSRC-STI-2008-00291, May 2008 (doi: 10.2172/935436).

102. Steimke, J. L., Steeper, T. J., and Herman, D. T. "Prevention of sulfur formation in hybrid sulfur electrolyzer," paper presented at the 2009 AIChE Annual Meeting, Nashville, TN, USA, November 8-13, 2009.

103. Sivasubramanian, P., Ramasamy, R. P., Freire, F. J., Holland, C. E., and Weidner, J. W. "Electrochemical hydrogen production from thermochemical cycles using a proton exchange membrane electrolyzer," *International Journal of Hydrogen Energy* 32(4), 463-468 (2007).

104. Staser, J., Ramasamy, R. P., Sivasubramanian, P., and Weidner, J. W. "Effect of water on the electrochemical oxidation of gas-phase SO_2 in a PEM electrolyzer for H_2 production," *Electrochemical and Solid-State Letters* **10**(11), E17-E19 (2007).

105. Staser, J. A., Norman, K., Fujimoto, C. H., Hickner, M. A., and Weidner, J. W. "Transport properties and performance of polymer electrolyte membranes for the hybrid sulfur electrolyzer," *Journal of the Electrochemical Society* **156**(7), B842-B847 (2009).

106. Staser, J. A., and Weidner, J. W. "Effect of SO_2 crossover on hydrogen and sulfuric acid production in a PEM electrolyzer," *ECS Transactions* **19**(10), 67-75 (2009).

107. Staser, J. A., and Weidner, J. W. "Sulfur dioxide crossover during the production of hydrogen and sulfuric acid in a PEM electrolyzer," *Journal of the Electrochemical Society* **156**(7), B836-B841 (2009).

108. Staser, J. A., and Weidner, J. W. "Effect of water transport on the production of hydrogen and sulfuric acid in a PEM electrolyzer," *Journal of the Electrochemical Society* **156**(1), B16-B21 (2009).

109. Staser, J. A., Gorensek, M. B., and Weidner, J. W. "Quantifying individual potential contributions of the hybrid sulfur electrolyzer," submitted to *Journal of the Electrochemical Society*.

110. Juda, W., and Moulton, D. M. "Effect of low-cost electrolytic hydrogen on the generation of basic chemicals," *Chemical Engineering Progress, Symposium Series* **63**(71), 59-62 (1967).

111. Hood, G. C., and Reilly, C. A. "Ionization of strong electrolytes. V. Proton magnetic resonance in sulfuric acid," *The Journal of Chemical Physics* **27**(5), 1126-1128 (1957).

112. Young, T. F., Maranville, L. F., and Smith, H. M. "Raman spectral investigations of ionic equilibria in solutions of strong electrolytes," in *The structure of electrolytic solutions*. Hamer, W. J. ed., Wiley, New York, 1959, pp. 35-63.

113. Clegg, S. L., Rard, J. A., and Pitzer, K. S. "Thermodynamic properties of 0–6 mol kg^{-1} aqueous sulfuric acid from 273.15 to 328.15 K," *Journal of the Chemical Society, Faraday Transactions* **90**(13), 1875-1894 (1994).

114. Clegg, S. L., and Brimblecombe, P. "Application of a multicomponent thermodynamic model to activities and thermal properties of 0-40 mol kg^{-1} aqueous sulfuric acid from <200 to 328 K," *Journal of Chemical & Engineering Data* **40**(1), 43-64 (1995).

115. Walrafen, G. E., Yang, W. H., Chu, Y. C., and Hokmabadi, M. S. "Structures of concentrated sulfuric acid determined from density, conductivity, viscosity, and Raman spectroscopic data," *Journal of Solution Chemistry* **29**(10), 905-936 (2000).

116. Wang, P., Anderko, A., Springer, R. D., and Young, R. D. "Modeling phase equilibria and speciation in mixed-solvent electrolyte systems: II. Liquid-liquid equilibria and properties of associating electrolyte solutions," *Journal of Molecular Liquids* **125**(1), 37-44 (2006).

117. Öztürk, I. T., Hammache, A., and Bilgen, E. "An improved process for H_2SO_4 decomposition step of the sulfur-iodine cycle," *Energy Conversion and Management* **36**(1), 11-21 (1995).

118. Moore, R. C., Gelbard, F., Parma, E. J., Vernon, M. E., Lenard, R. X., and Pickard, P. S. "A laboratory-scale sulfuric acid decomposition apparatus for use in hydrogen production cycles," *Proceedings: International Topical Meeting on Safety and Technology of Nuclear Hydrogen Production, Control, and Management , Boston, MA, USA, June 24-28, 2007*, pp. 161-166.

119. Koster, A., Matzner, H. D., and Nicholsi, D. R. "PBMR design for the future," *Nuclear Engineering and Design* **222**(2-3), 231-245 (2003).

120. Richards, M., Shenoy, A., Schultz, K., Brown, L., Harvego, E., McKellar, M., Coupey, J.-P., Reza, S. M. M., Okamoto, F., and Handa, N. "H2-MHR conceptual designs based on the sulphur–iodine process and high-temperature electrolysis," *International Journal of Nuclear Hydrogen Production and Applications* **1**(1), 36 - 50 (2006).

121. "Aspen Plus." Version 7.0 (22.0.4191), Aspen Technology, Inc., Burlington, MA, USA, 1981-2008.

122. "Aspen Energy Analyzer." Version 7.0 (22.0.0.5705), Aspen Technology, Inc., Burlington, MA, USA, 1995-2008.

123. "JMP." Version 7.0.2, SAS Institute, Inc., Cary, NC, USA, 1989-2007.

124. "OLI Engine in Aspen Plus." Version 8.0, Revision 0, April 2008, ESP Build 58, OLI Systems, Inc., Morris Plains, NJ, USA, 1997-2008.

125. Miles, F. D., and Fenton, J. "The solubility of sulfur dioxide in sulfuric acid," *Journal of the Chemical Society, Transactions* **117**, 59-61 (1920).

126. Kuznetsov, D. A. "Study of the equilibrium pressures of sulfur dioxide over water and aqueous solutions of sulfuric acid (transl.)," *Zhurnal Khimicheskoi Promyshlennosti* **18**(22), 3-7 (1941).

127. Miles, F. D., and Carson, T. "Solubility of sulfur dioxide in fuming sulfuric acid," *Journal of the Chemical Society*, **1946**, 786-790.

128. Maass, C. E., and Maass, O. "Sulfur dioxide and its aqueous solutions. I. Analytical methods, vapor density and vapor pressure of sulfur dioxide. Vapor pressure and concentrations of the solutions," *Journal of the American Chemical Society* **50**(5), 1352-1368 (1928).

129. Spall, B. C. "Phase equilibriums in the system sulfur dioxide-water from 25-300°," *The Canadian Journal of Chemical Engineering* **41**, 79-83 (1963).

130. Van Berkum, J. G., and Diepen, G. A. M. "Phase equilibria in SO_2 + H_2O: the sulfur dioxide gas hydrate, two liquid phases, and the gas phase in the temperature range 273 to 400 K and at pressures up to 400 MPa," *The Journal of Chemical Thermodynamics* **11**(4), 317-334 (1979).

131. Weidner, J. W. "Personal Communication." Email dated June 17, 2009.

TABLE 19.1 Candidate PEM Materials for the SDE Application

Membrane description	Source
Perfluorinated sulfonic acid (PFSA)	DuPont
Polybenzimidizole (PBI)	BASF (Germany)
Sulfonated Diels-Alder polyphenylene (SDAPP)	Sandia National Laboratories
Stretched recast PFSA	Case Western Reserve University
Nafion®/fluorinated ethylene propylene (FEP) blends	Case Western Reserve University
Treated PFSA	Giner Electrochemical Systems, LLC
Perfluorocyclobutane-biphenyl vinyl ether (BPVE)	Clemson University
Perfluorocyclobutane-biphenyl vinyl ether-hexafluoroisopropylidene (BPVE-6F)	Clemson University

TABLE 19.2. HyS Flowsheet Stream Table [97]

Stream ID	Molar flow rates, kmol/sec						Temperature,		Pressure, bar	Phase
	H_2O	H_2SO_4	SO_2	O_2	H_2	Total	°C	°K		
1	10	0	0	0	0.00235	10.0024	73.20	346.35	21	L
2	27.4794	3.88405	2.5	0.00527	0	37.7528	78.77	351.92	21	L
3	9	0	0	0	1.00235	10.0024	100.00	373.15	20	L + V
4	9	0	0	0	1.00235	10.0024	76.96	350.11	20	L + V
5	0.02185	0	0	0	1.00004	1.02189	76.96	350.11	20	V
6	0	0	0	0	1.00004	1.00004	40.00	313.15	20	V
7	8.97815	0	0	0	0.00231	8.98046	76.96	350.11	20	L
8	0.02185	0	0	0	0	0.02185	40.00	313.15	20	L
9	1	0	0	0	0	1	40.00	313.15	20	L
10	10	0	0	0	0.00231	10.0023	73.19	346.34	20	L
11	26.4794	4.88405	1.5	0.00527	0	37.7528	100.00	373.15	20	L + V
12	5.42394	1.00043	0.30725	0.00108	0	7.73314	100.00	373.15	20	L + V
13	5.42394	1.00043	0.30725	0.00108	0	7.73314	84.08	357.23	1.01325	L + V
14	5.33174	1.00043	0.02004	3.9E-07	0	7.35265	84.08	357.23	1.01325	L
15	5.33174	1.00043	0.02004	3.9E-07	0	7.35265	80.38	353.53	0.30198	L + V
16	5.29406	1.00043	0.00263	2.9E-10	0	7.29756	80.38	353.53	0.30198	L
17	5.29406	1.00043	0.00263	2.9E-10	0	7.29756	66.96	340.11	0.11	L + V
18	5.29406	1.00043	0.00263	2.9E-10	0	7.29756	94.41	367.56	0.11	L + V
19	3.7702	2.07782	6.7E-12	2E-21	0	7.92584	122.87	396.02	0.13	L
20	3.7702	2.07782	6.7E-12	0	0	7.92584	123.63	396.78	86	L
21	4.77063	1.07739	1.00043	0.50021	0	8.42605	254.70	527.85	86	L + V
22	4.30695	1.07739	0.23587	0.00844	0	6.70604	254.70	527.85	86	L
23	4.30695	1.07739	0.23587	0.00844	0	6.70604	233.42	506.57	21	L + V
24	4.03002	1.07739	0.04733	8.9E-05	0	6.23222	233.42	506.57	21	L
25	4.03002	1.07739	0.04733	8.9E-05	0	6.23222	147.33	420.48	1.01325	L + V
26	3.13019	1.07739	0.00035	1.4E-08	0	5.28532	147.33	420.48	1.01325	L
27	3.13019	1.07739	0.00035	1.4E-08	0	5.28532	118.57	391.72	0.30198	L + V
28	2.87261	1.07739	3.7E-06	2.4E-12	0	5.02739	118.57	391.72	0.30198	L
29	2.87261	1.07739	3.7E-06	2.4E-12	0	5.02739	100.50	373.65	0.13	L + V
30	2.87261	1.07739	3.7E-06	2.4E-12	0	5.02739	114.62	387.77	0.13	L + V
31	0.46368	5.5E-06	0.76455	0.49177	0	1.72001	254.70	527.85	86	V
32	0.46368	5.5E-06	0.76455	0.49177	0	1.72002	110.50	383.65	86	L + V
33	0.46368	5.5E-06	0.76455	0.49177	0	1.72002	76.96	350.11	86	L + V
34	0.46368	5.5E-06	0.76455	0.49177	0	1.72002	40.00	313.15	86	L + V
35	0.08967	1.8E-07	0.65507	0.00123	0	0.74597	40.00	313.15	86	L
36	0.08967	1.8E-07	0.65507	0.00123	0	0.74597	41.78	314.93	21	L + V

37	0.08966	1.8E-07	0.65459	0.00025	0	0.74451	41.78	314.93	21	L
38	0.37282	5.3E-06	0.03946	0.00066	0	0.41296	40.00	313.15	86	L
39	0.37282	5.3E-06	0.03946	0.00066	0	0.41296	40.99	314.14	21	L + V
40	0.37282	5.3E-06	0.03922	0.00014	0	0.41218	40.99	314.14	21	L
41	0.00119	0	0.07002	0.48988	0	0.56109	40.00	313.15	86	V
42	0.00119	0	0.07002	0.48988	0	0.56109	15.50	288.65	21	L + V
43	0.0006	0	4.7E-05	3.8E-07	0	0.00065	15.50	288.65	21	L
44	0.00059	0	0.06997	0.48988	0	0.56044	15.50	288.65	21	V
45	3.5E-06	4.3E-26	0.00025	0.00052	0	0.00077	40.99	314.14	21	V
46	6.9E-06	1E-25	0.00048	0.00098	0	0.00146	41.78	314.93	21	V
47	0.27692	1.3E-06	0.18854	0.00835	0	0.47382	233.42	506.57	21	V
48	21.0554	3.88362	1.19275	0.00419	0	30.0196	100.00	373.15	20	L + V
49	21.0554	3.88362	1.19275	0.00419	0	30.0196	80.00	353.15	20	L
50	21.0554	3.88362	1.19275	0.00419	0	30.0196	80.01	353.16	21	L
51	27.4794	3.88405	2.5	0.00524	0	37.7527	84.71	357.86	21	L
52	0.0922	2E-11	0.28721	0.00108	0	0.38049	84.08	357.23	1.01325	V
53	0.0922	2E-11	0.28721	0.00108	0	0.38049	40.00	313.15	1.01325	L + V
54	0.89983	6.6E-07	0.04698	8.9E-05	0	0.9469	147.33	420.48	1.01325	V
55	0.89983	6.6E-07	0.04698	8.9E-05	0	0.9469	110.50	383.65	1.01325	L + V
56	0.89983	6.6E-07	0.04698	8.9E-05	0	0.9469	76.96	350.11	1.01325	L + V
57	0.89983	6.6E-07	0.04698	8.9E-05	0	0.9469	40.00	313.15	1.01325	L + V
58	0.02674	2.3E-24	0.33759	0.00117	0	0.3655	40.00	313.15	1.01325	V
59	1.9E-05	0	0.00541	0.00116	0	0.00659	40.00	313.15	21	L + V
60	1.9E-05	0	0.0048	1.2E-06	0	0.00482	40.00	313.15	21	L
61	0.00936	0	0.33626	1E-05	0	0.34562	41.20	314.35	21	L
62	0.01738	0	0.00073	3.5E-09	0	0.01811	40.00	313.15	2.78324	L
63	0.01738	0	0.00073	3.5E-09	0	0.01811	41.11	314.26	21	L
64	0.00934	0	0.33146	9.2E-06	0	0.3408	40.00	313.15	7.64513	L
65	0.00934	0	0.33146	9.2E-06	0	0.3408	41.22	314.37	21	L
66	3.2E-07	0	0.00061	0.00116	0	0.00177	40.00	313.15	21	V
67	0.96665	6.6E-07	0.01365	6.1E-08	0	0.9803	40.00	313.15	1.01325	L
68	0.96665	6.6E-07	0.01365	6.1E-08	0	0.9803	40.31	313.46	21	L
69	0.03768	6.4E-12	0.01741	3.9E-07	0	0.0551	80.38	353.53	0.30198	V
70	0.03768	6.4E-12	0.01741	3.9E-07	0	0.0551	40.00	313.15	0.30198	L + V
71	0.25758	1E-07	0.00035	1.4E-08	0	0.25793	118.57	391.72	0.30198	V
72	0.25758	1E-07	0.00035	1.4E-08	0	0.25793	76.96	350.11	0.30198	L + V
73	0.25758	1E-07	0.00035	1.4E-08	0	0.25793	40.00	313.15	0.30198	L
74	0.28961	1E-07	0.00106	2.8E-11	0	0.29067	40.61	313.76	0.30198	L
75	0.28961	1E-07	0.00106	2.8E-11	0	0.29067	41.14	314.29	21	L
76	0.0059	1.2E-25	0.01745	4.1E-07	0	0.02335	40.61	313.76	0.30198	V
77	0.02335	0	0	0	0	0.02335	169.99	443.14	7.91	L + V

78	0.02925	0	0.01745	4.1E-07	0	0.0467	93.77	366.92	1.01325	V
79	0.0279	0	0.0004	1.2E-11	0	0.0283	40.00	313.15	1.01325	L
80	0.00135	0	0.01706	4.1E-07	0	0.0184	40.00	313.15	1.01325	V
81	4.39285	6.9E-35	0.00185	4.9E-13	0	4.3947	40.02	313.17	0.09	L
82	4.39285	0	0.00185	4.9E-13	0	4.3947	40.21	313.36	21	L
83	0.00361	5.2E-35	0.00079	3E-10	0	0.0044	40.02	313.17	0.09	V
84	0.0044	0	0	0	0	0.0044	169.99	443.14	7.91	L + V
85	0.00801	0	0.00079	3E-10	0	0.0088	95.05	368.20	0.30198	V
86	0.00777	0	2.9E-05	1.3E-14	0	0.0078	40.00	313.15	0.30198	L
87	0.00777	0	2.9E-05	1.3E-14	0	0.0078	40.04	313.19	1.01325	L
88	0.03567	0	0.00042	1.2E-11	0	0.03609	40.03	313.18	1.01325	L
89	0.00025	0	0.00076	3E-10	0	0.001	40.00	313.15	0.30198	V
90	0.00228	1.4E-34	0.00413	0.50024	0	0.50665	41.12	314.27	21	V
91	0	0	0	0.50024	0	0.50024	40.00	313.15	21	V
92	5.92438	2.1E-06	0.27327	0.00116	0	6.19882	82.33	355.48	21	L
93	0.00228	0	0.00413	0	0	0.00641	40.00	313.15	21	L
94	2.9E-05	7.6E-16	0.00098	0.00051	0	0.00152	84.71	357.86	21	V
MAKEUP	0.00749	0.00042	0	0	0	0.00834	40.00	313.15	21	L

TABLE 19.3 HyS Flowsheet Heat Exchangers [97]

Block ID	Duty, MW_{th}	Temperature, °C (K)		Heat Exchanged With:
		Inlet	Outlet	
CO-01/Stage 1 Cooler	-2.290	138.02 (411.2)	40.0 (313)	Cooling Water
CO-01/Stage 2 Cooler	-9.109	137.79 (410.9)	40.0 (313)	Cooling Water
CO-01/Stage 3 Cooler	-0.132	143.76 (416.9)	40.0 (313)	Cooling Water
DR-01	-2.045	76.96 (350.1)	40.0 (313)	Cooling Water
DR-02	-0.197	41.12 (314.3)	40.0 (313)	Cooling Water
HX-01	-17.688	100.00 (373.0)	76.96 (350.1)	HX-02
HX-02	130.486	66.96 (340.1)	94.41 (367.6)	HX-01, HX-04B, HX-05, HX-06, HX08B, HX-10A
HX-03	31.777	100.50 (373.7)	114.62 (387.8)	HX-04A, HX-08A
HX-04A	-30.543	254.70 (527.9)	110.50 (383.7)	HX-03
HX-04B	-8.400	110.50 (383.7)	76.96 (350.1)	HX-02
HX-04C	-6.243	76.96 (350.1)	40.0 (313)	Cooling Water
HX-05	-47.903	100.00 (373.0)	80.00 (353.0)	HX-02
HX-06	-18.686	84.71 (357.9)	78.77 (351.9)	HX-02
HX-07	-3.702	84.08 (357.2)	40.0 (313)	Cooling Water
HX-08A	-1.234	147.33 (420.5)	110.50 (383.7)	HX-03
HX-08B	-37.440	110.50 (383.7)	76.96 (350.1)	HX-02
HX-08C	-4.021	76.96 (350.1)	40.0 (313)	Cooling Water
HX-09	-1.476	80.38 (353.5)	40.0 (313)	Cooling Water
HX-10A	-0.368	118.57 (391.7)	76.96 (350.1)	HX-02
HX-10B	-11.503	76.96 (350.1)	40.0 (313)	Cooling Water
HX-11	-1.310	93.77 (366.9)	40.0 (313)	Cooling Water
HX-12	-0.354	95.05 (368.2)	40.0 (313)	Cooling Water
RX-01	340.280	123.63 (396.8)	254.70 (527.9)	High-Temp. Source
TO-01 Reboiler	75.482	102.74 (375.9)	122.87 (396.0)	Low-Temp. Source
TO-01 Condenser	-210.542	44.80 (318.0)	40.0 (313)	Cooling Water

TABLE 19.4 HyS Flowsheet Electrolyzers, Pumps, and Compressors [97]

Block ID	Work, MW_e
EL-01	115.782
CO-01/Stage 1	1.464
CO-01/Stage 2	1.357
CO-01/Stage 3	0.025
PP-01	0.022
PP-02	1.836
PP-03	0.071
PP-04	0.002
PP-05	0.028
PP-06	0.055
PP-07	0.021
PP-08	0.212
PP-09	0.00003

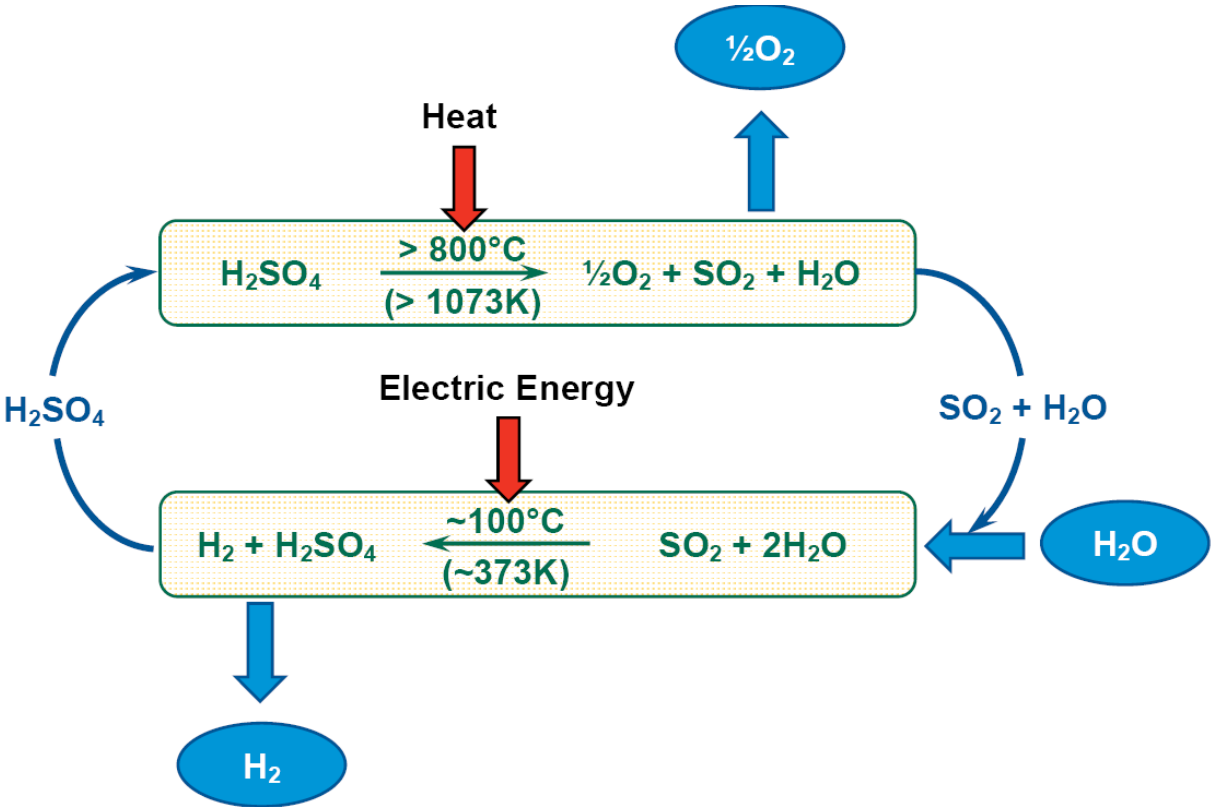

Figure 19.1 The Hybrid Sulfur Cycle.

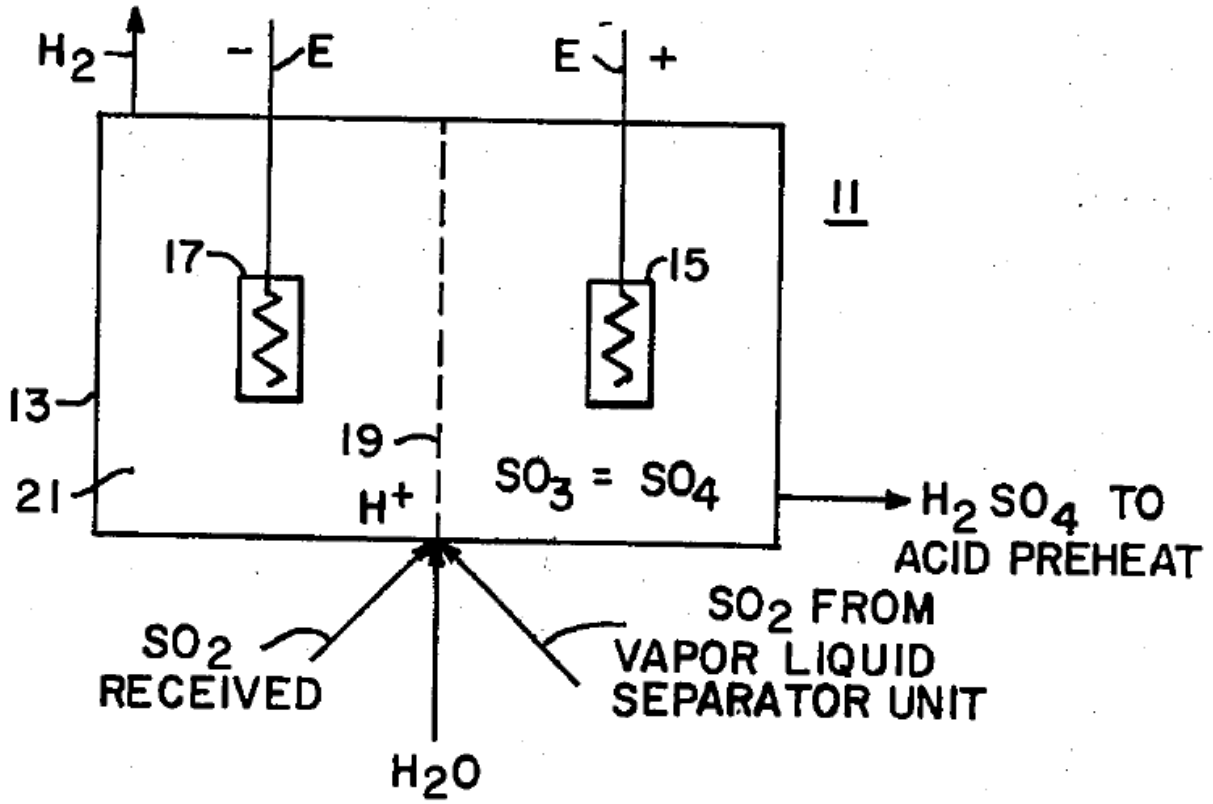

Figure 19.2 SO_2-depolarized Electrolyzer Cell in the Original Westinghouse Patent [1].

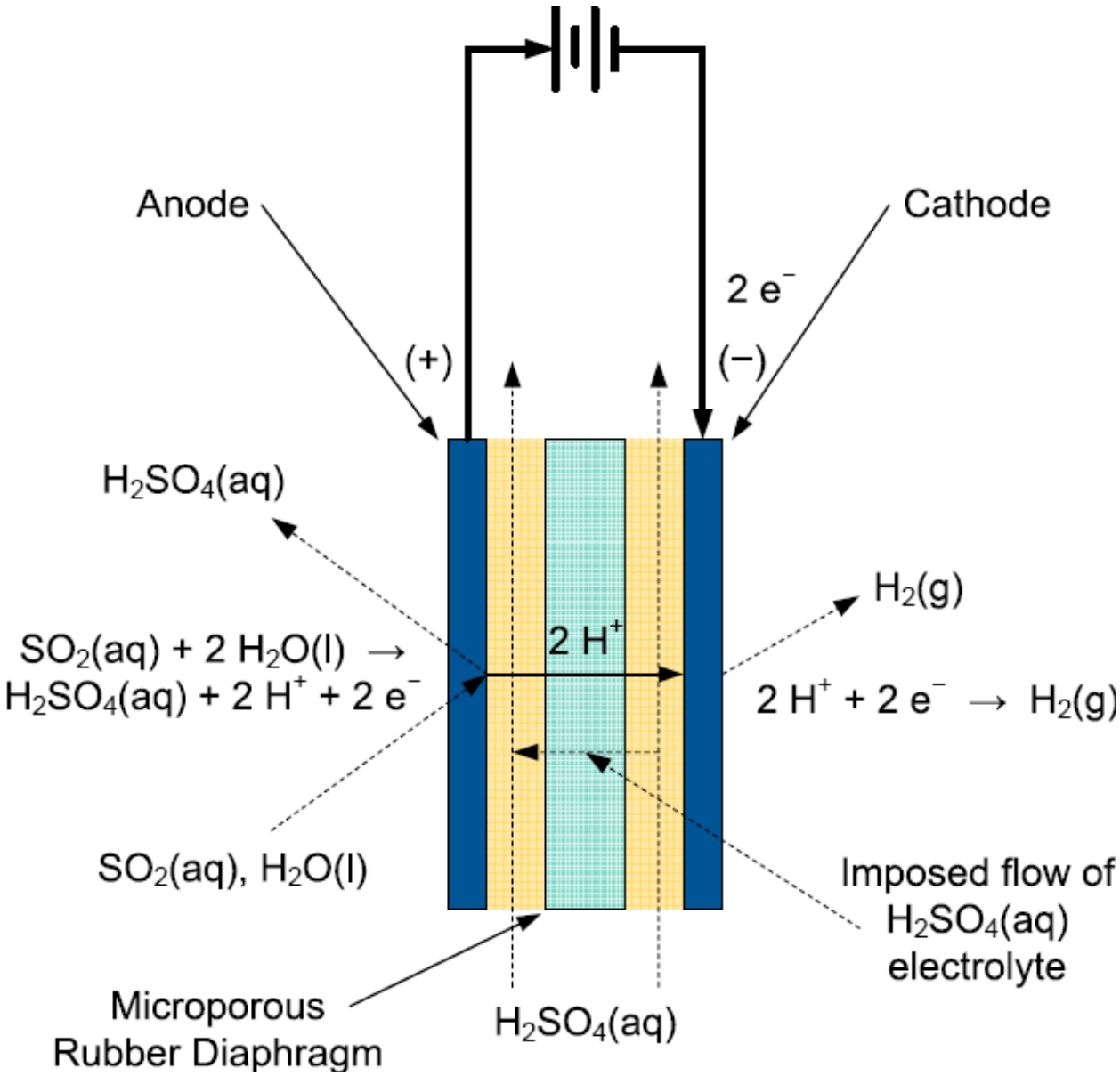

Figure 19.3 Westinghouse SO_2-depolarized Electrolyzer Cell.

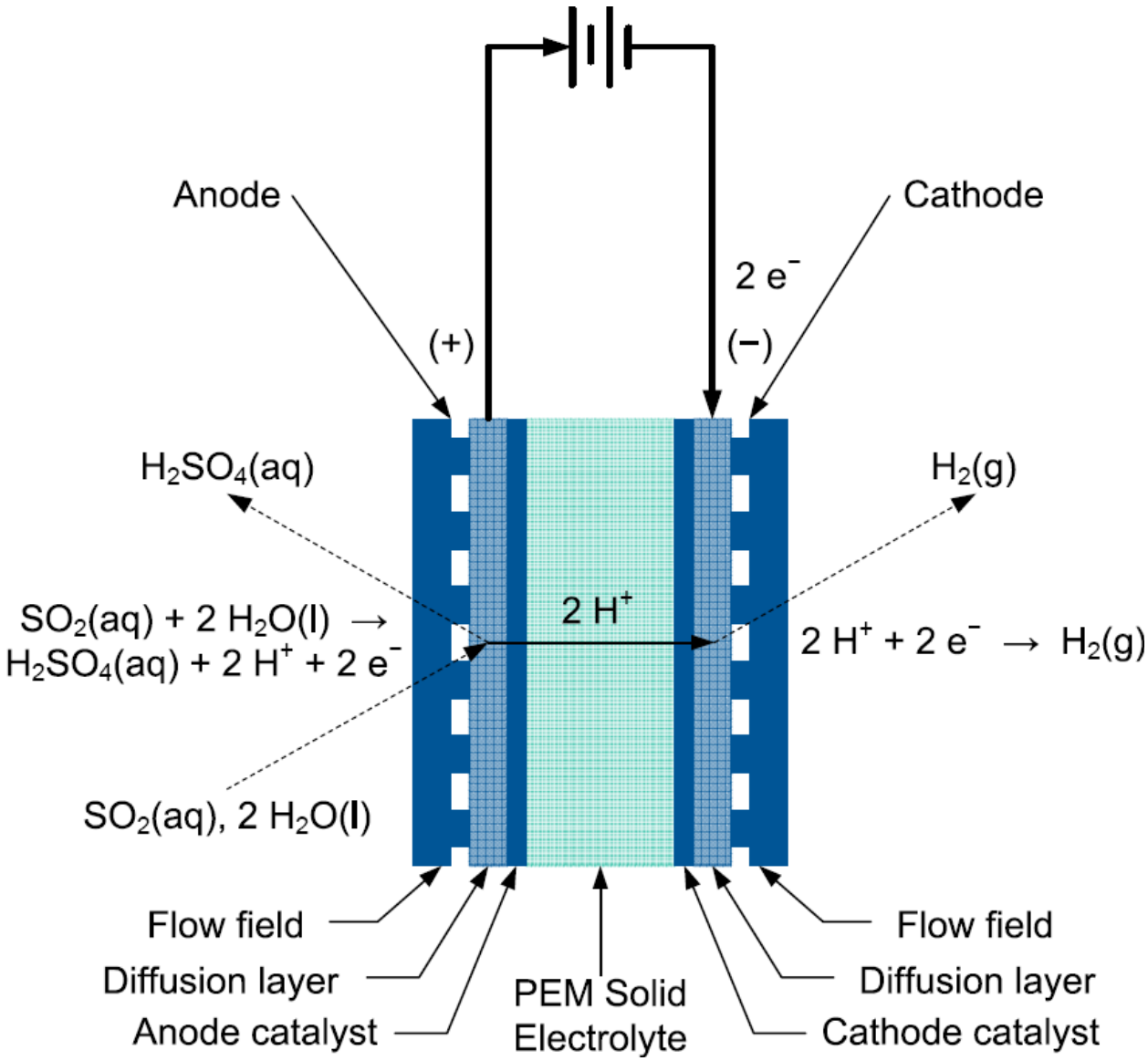

Figure 19.4 SRNL PEM SO_2-depolarized Electrolyzer Cell; SO_2 Dissolved in Sulfuric Acid under Pressure Is Fed to the Anode, While Water Is Fed to the Cathode.

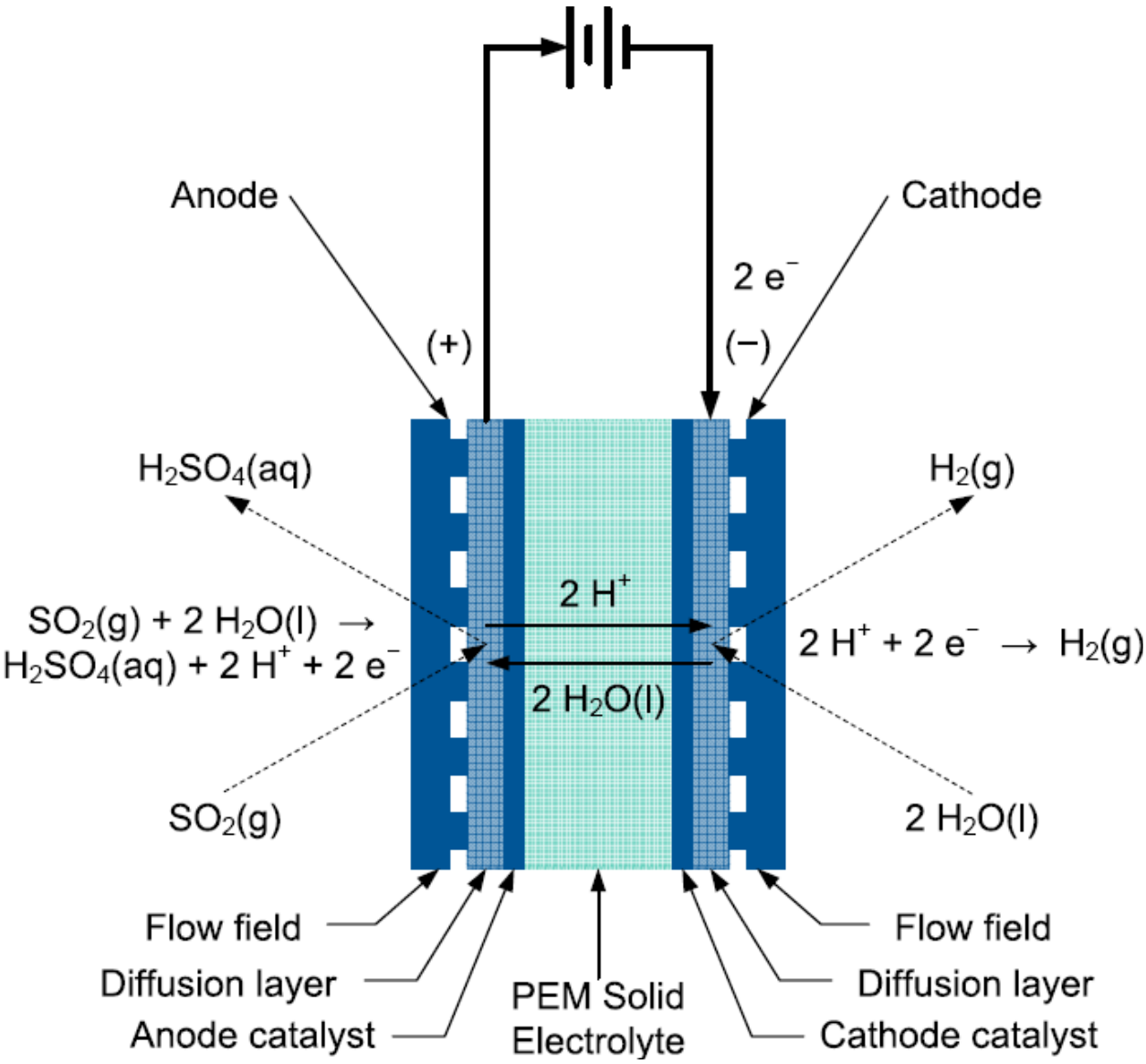

Figure 19.5 USC PEM SO_2-depolarized Electrolyzer Cell; Gaseous SO_2 Is Fed to the Anode, While Water Is Fed to the Cathode.

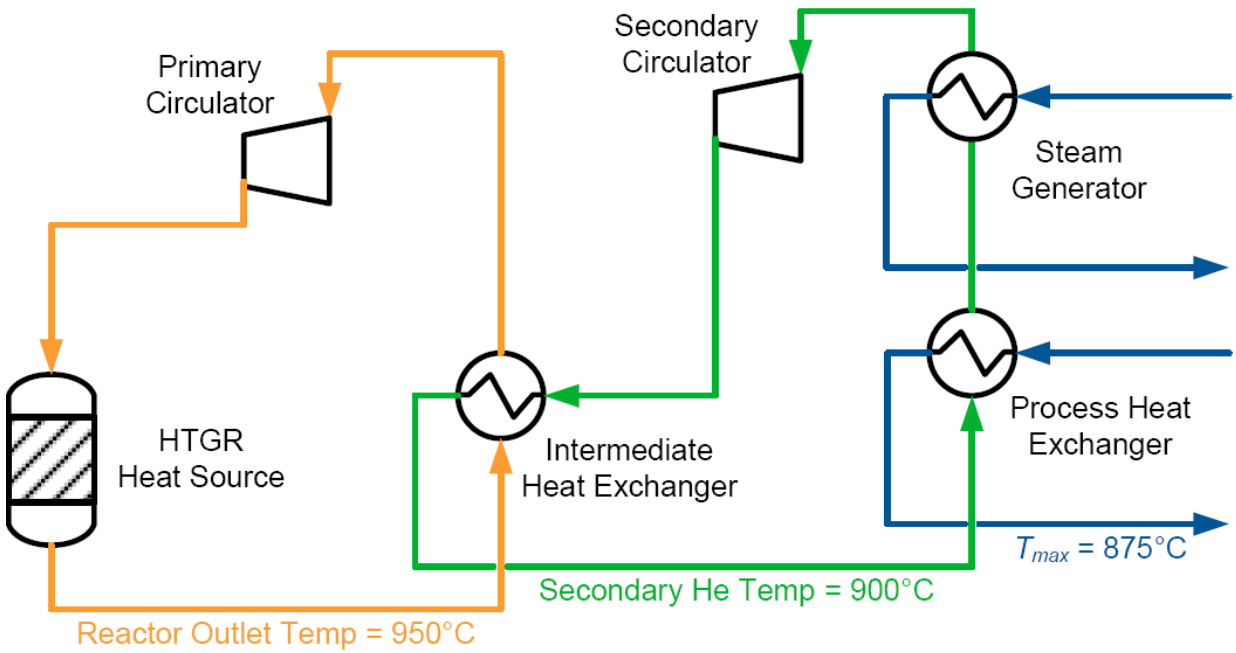

Figure 19.6 Schematic Diagram for an HTGR-heated Water-splitting Process Showing the Relationship between the Heat Source and the Process; in This Example, the Reactor Outlet Temperature is 950°C, with a 50°C Temperature Difference between the Primary and Secondary Loops, and a Minimum Temperature Difference for Helium-to-process Fluid Heat Transfer of 25°C, Resulting in a Peak Process Temperature of 875°C.

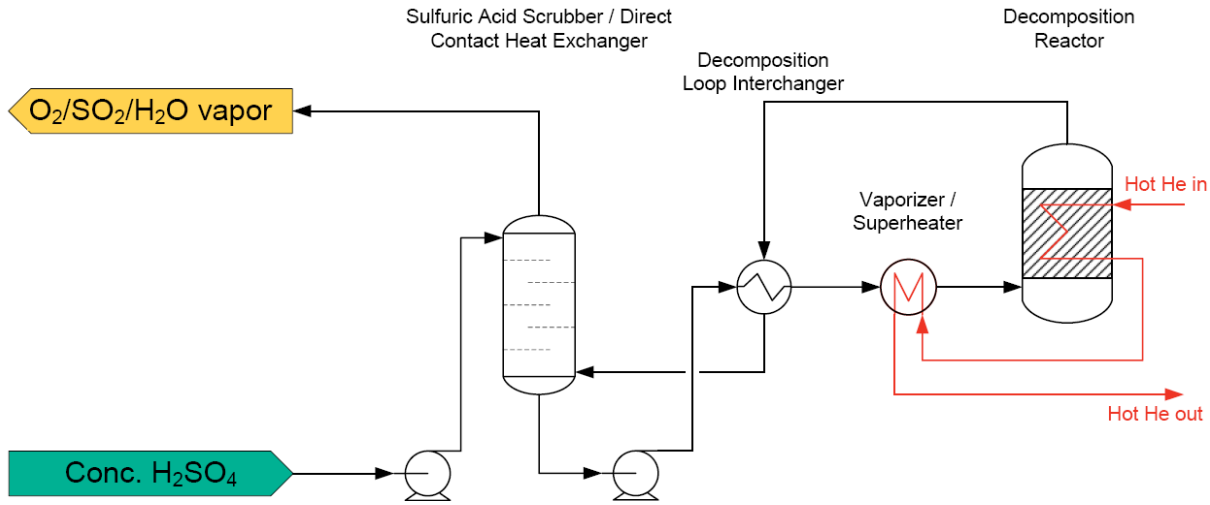

Figure 19.7 Öztürk et al. High-temperature Sulfuric Acid Decomposition Loop.

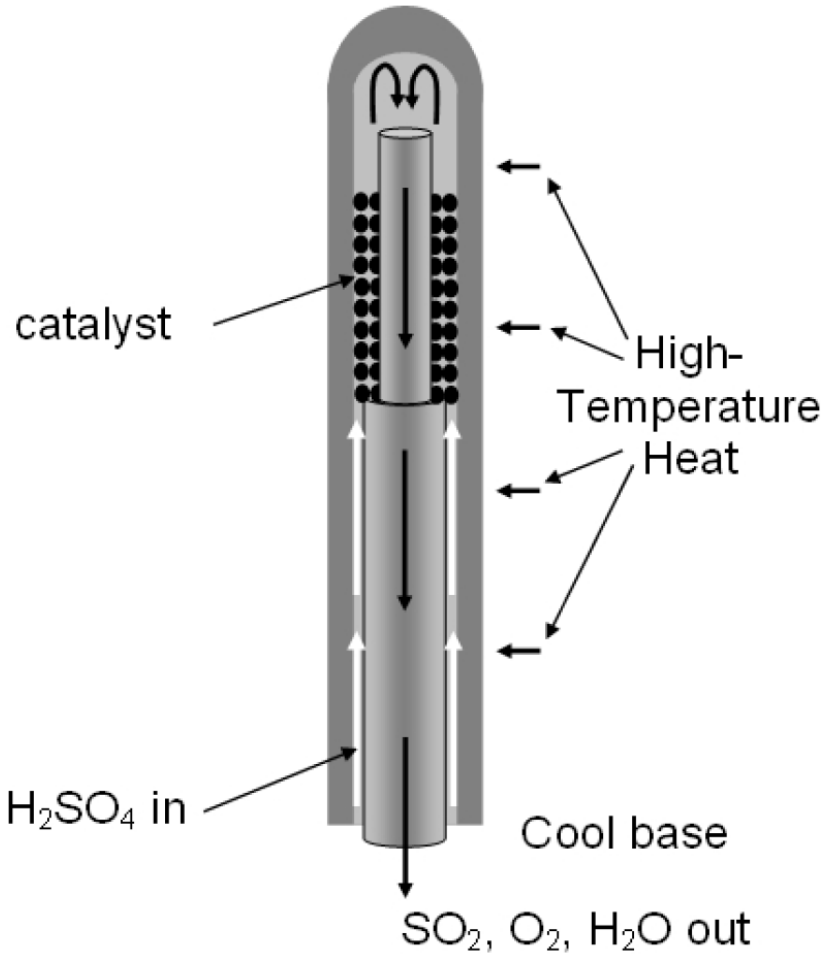

Figure 19.8 High-temperature Sulfuric Acid Decomposition Bayonet Reactor [98]; the Exterior Is Heated by Secondary Helium Heat Transfer Fluid Flowing from the Top, with the Lower End Insulated to Facilitate Recuperation and Allow Low-temperature Fluid Connections.

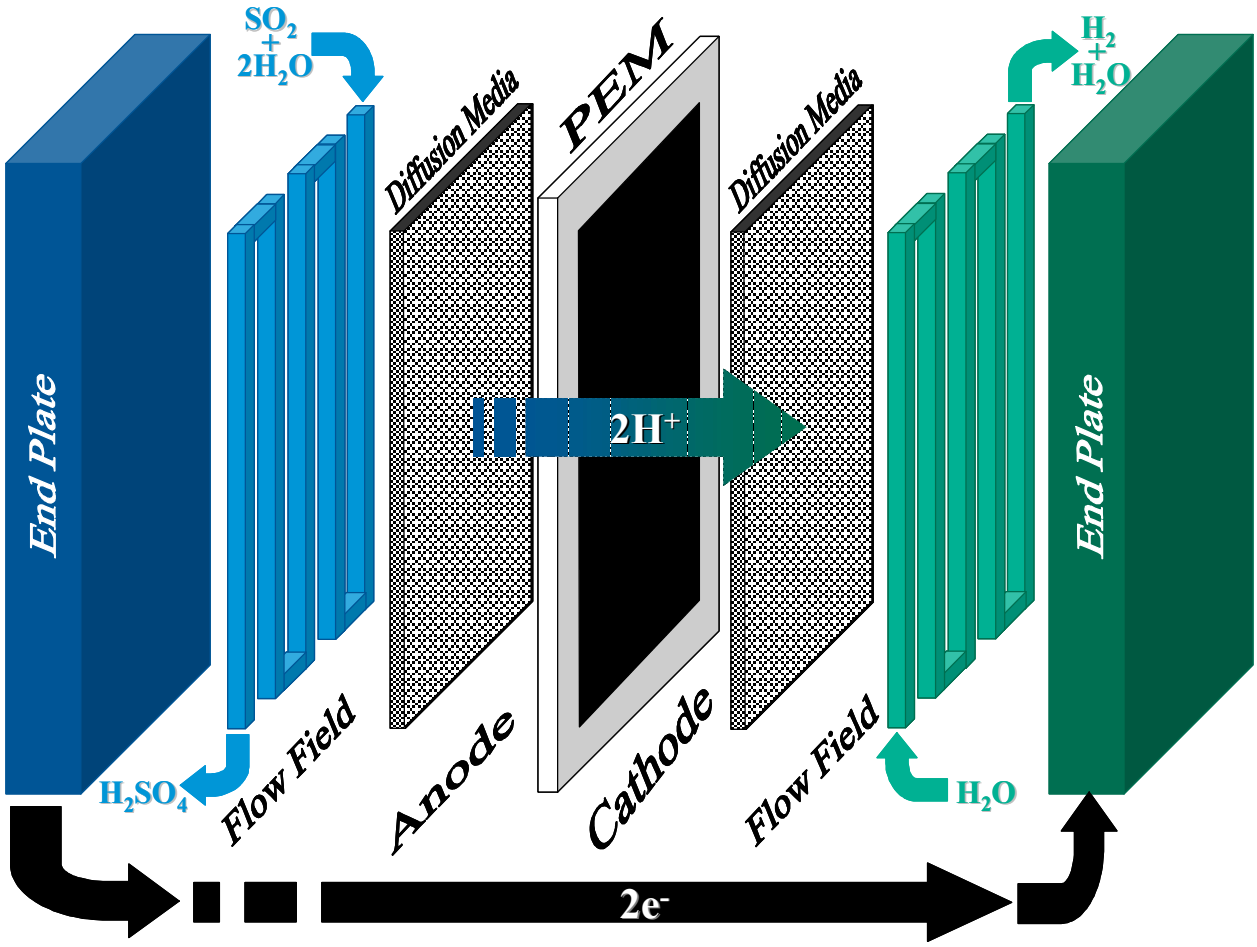

Figure 19.9 Major Components of a PEM-type SO_2-depolarized Electrolyzer.

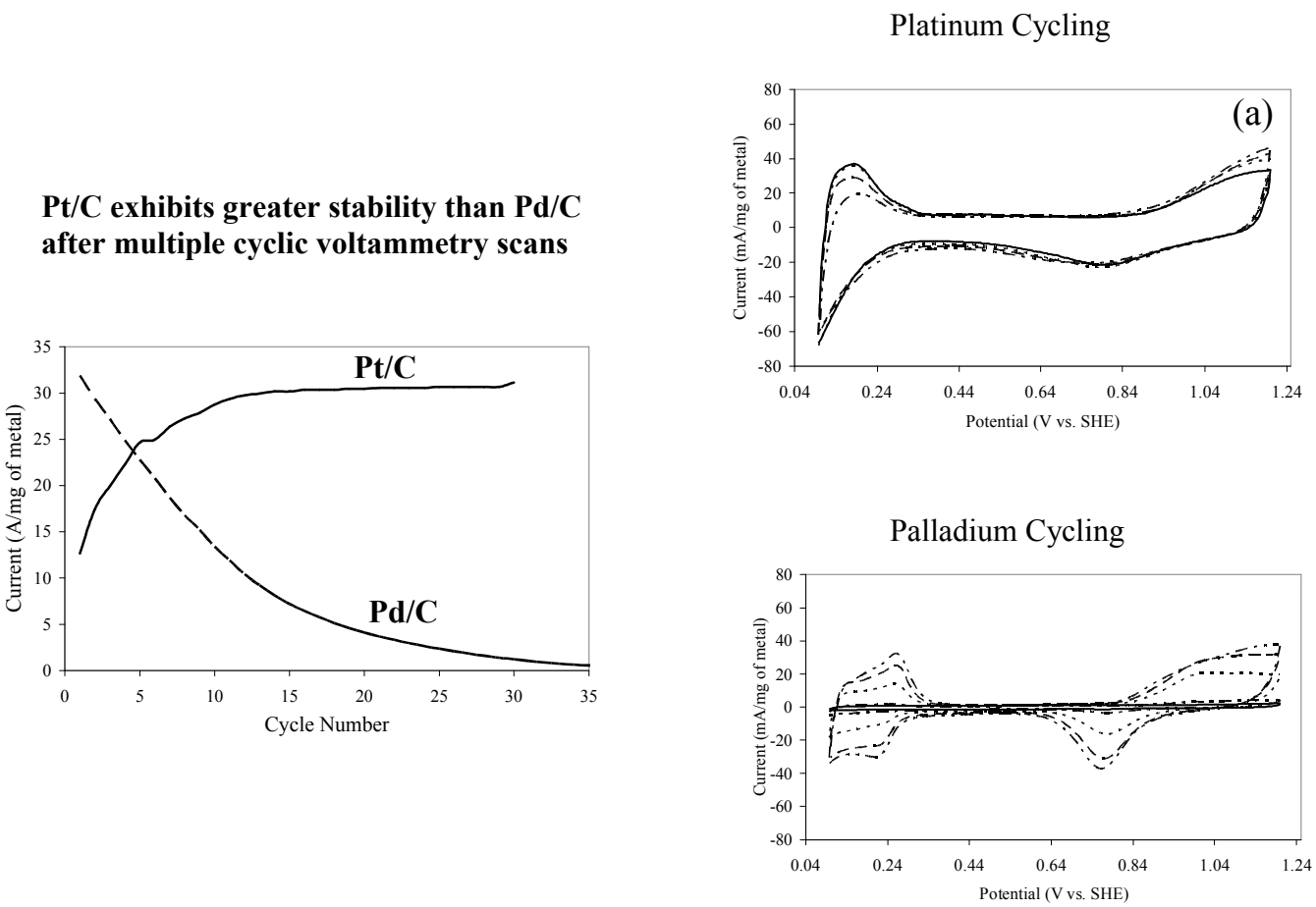

Figure 19.10 Catalytic Activity and Stability of Pt/C and Pd/C for SO_2 Oxidation [91].

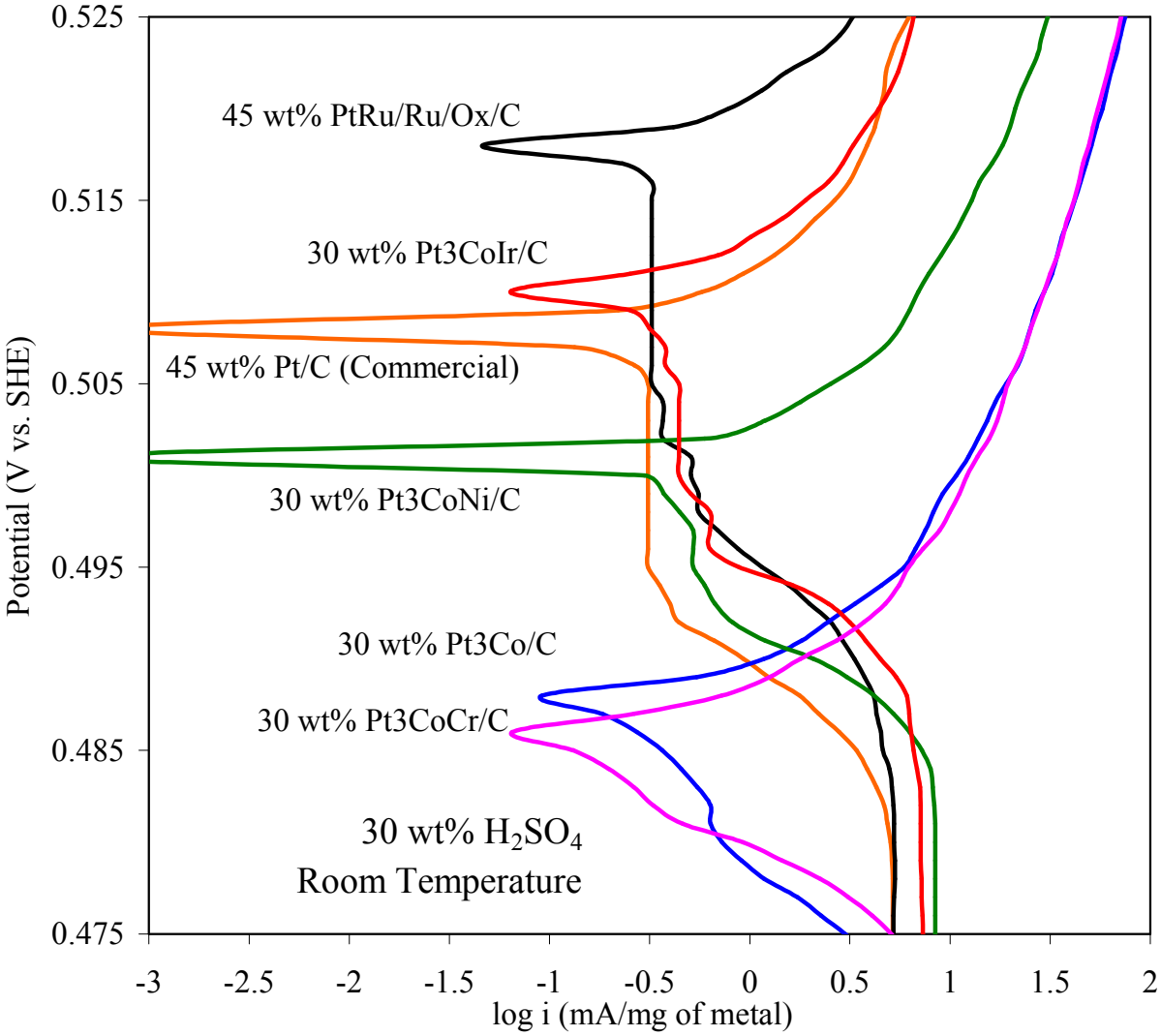

Figure 19.11 Catalytic Activity of Pt-based Catalysts for the Oxidation of SO_2 in 30-wt % Sulfuric Acid and at Room Temperature [101].

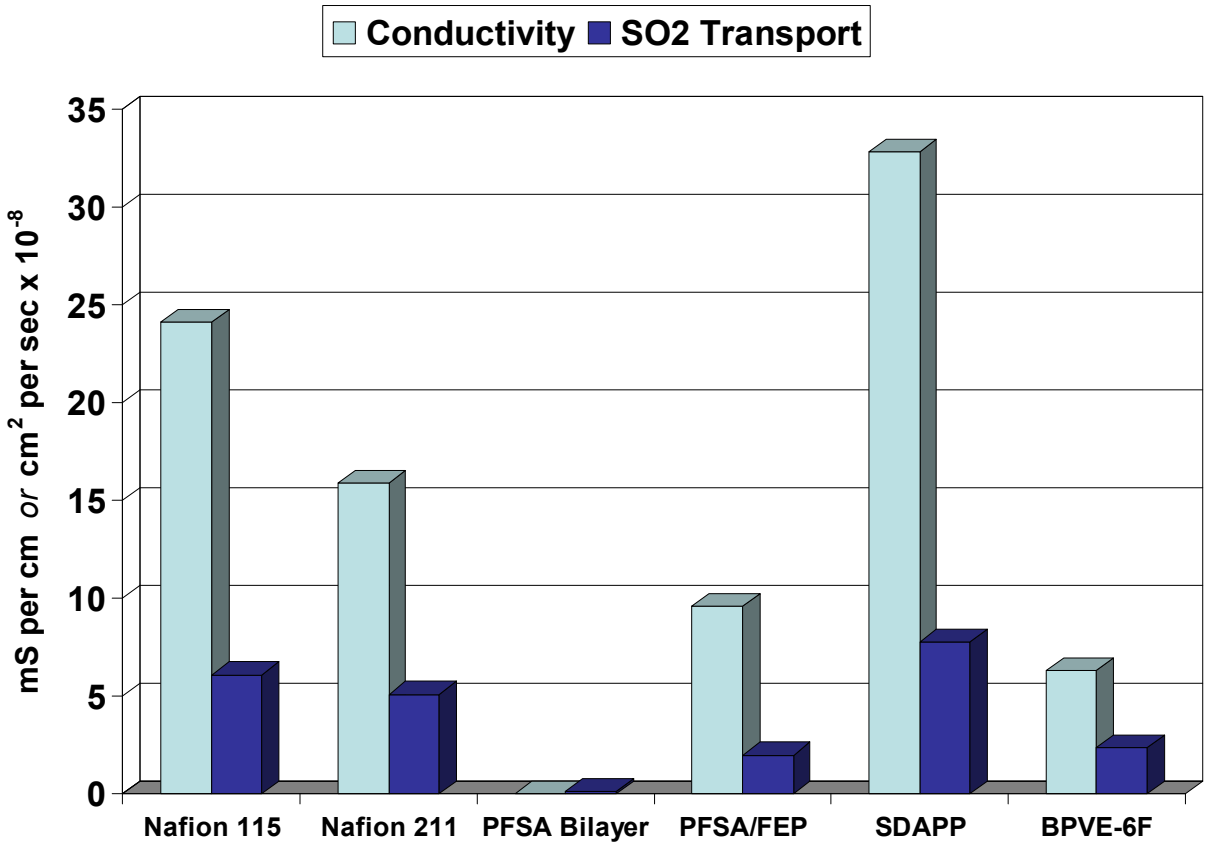

Figure 19.12 Proton Exchange Membrane Results Showing Ionic Conductivity and SO_2 Diffusion [93].

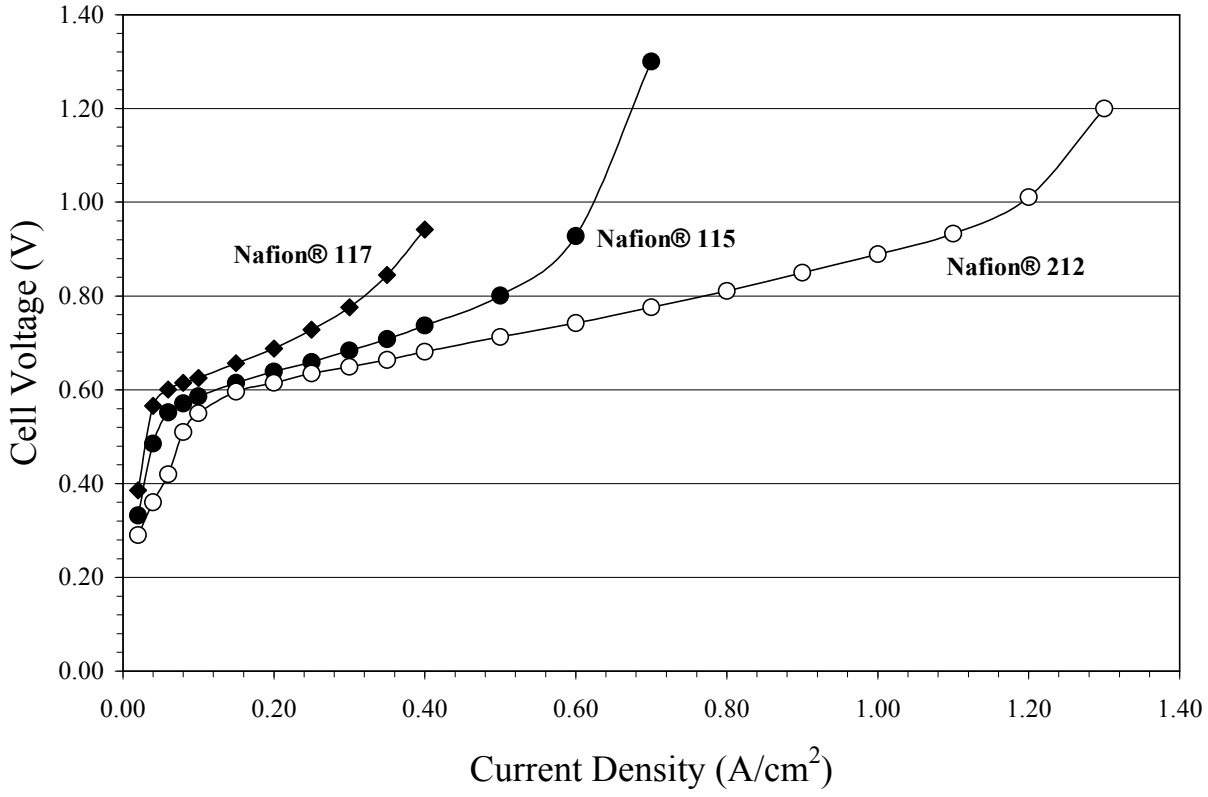

Figure 19.13 Polarization Curves for Nafion® 212, 115, and 117 Membranes [104].

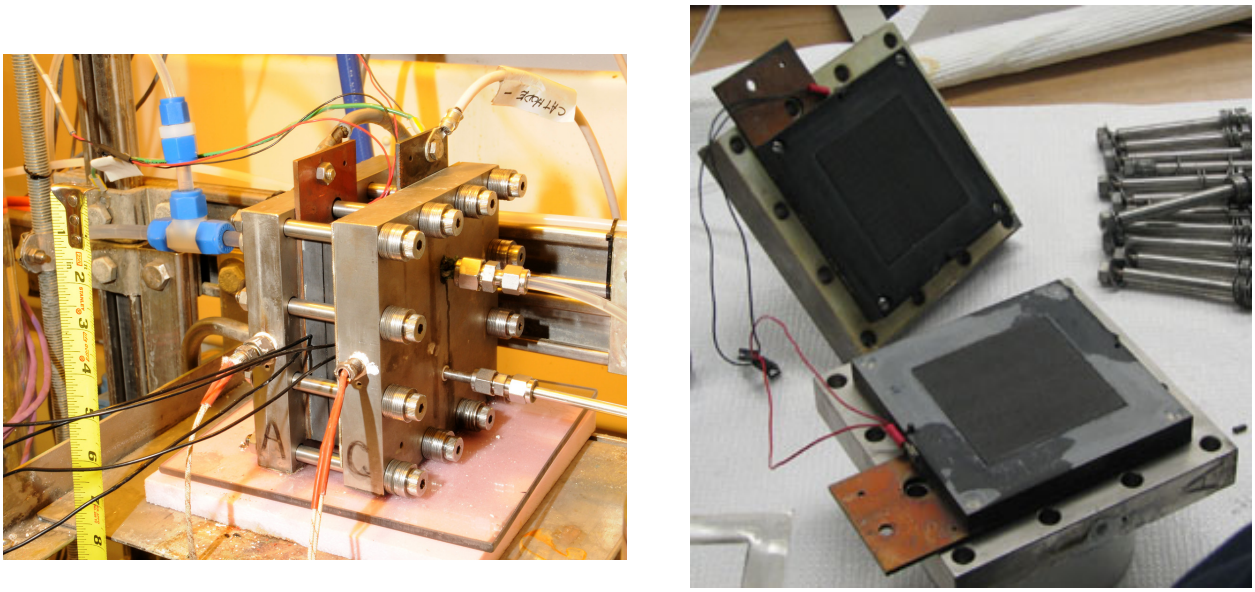

Figure 19.14 The SRNL Single-cell SO_2-depolarized Electrolyzer.

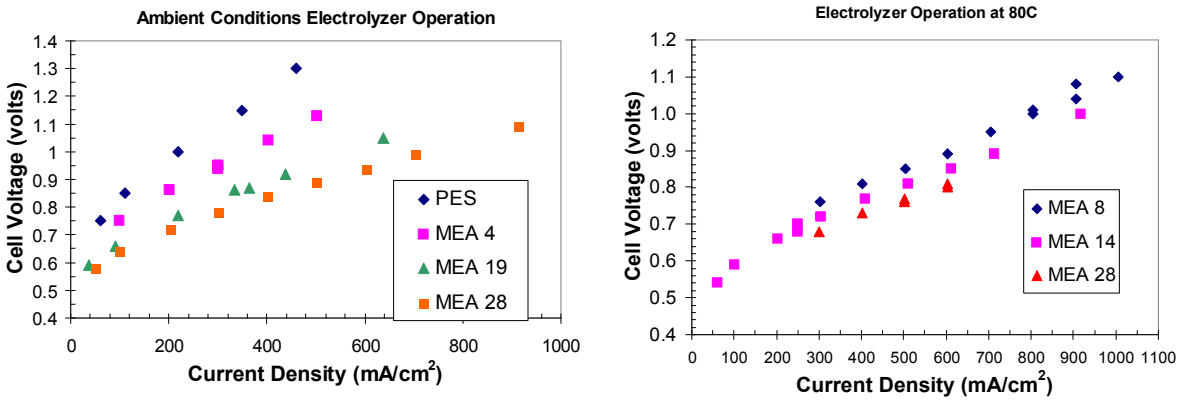

Figure 19.15 Representative Polarization Curve for the SRNL Single-cell Electrolyzer [94].

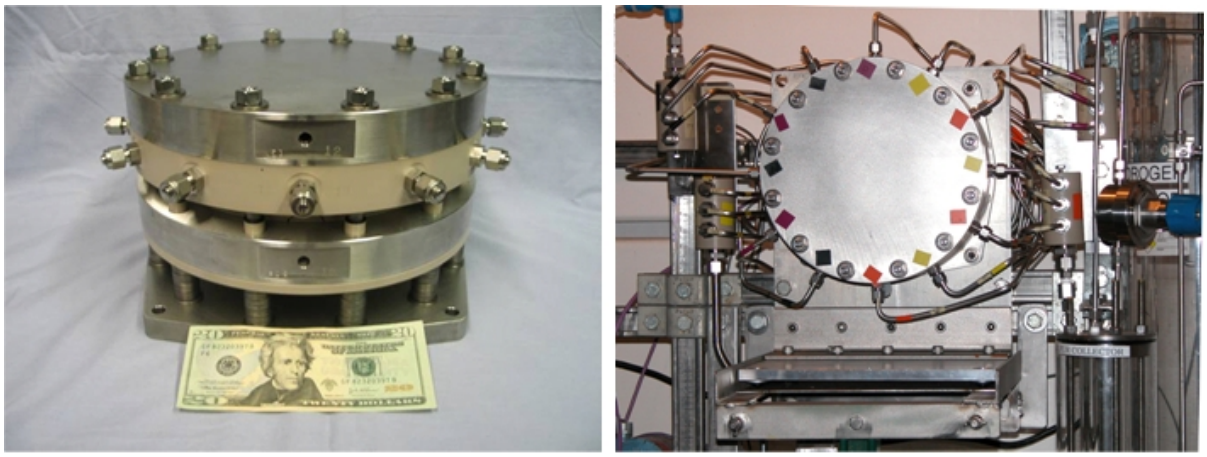

Figure 19.16 The SRNL Three-cell SO_2-depolarized Electrolyzer [92].

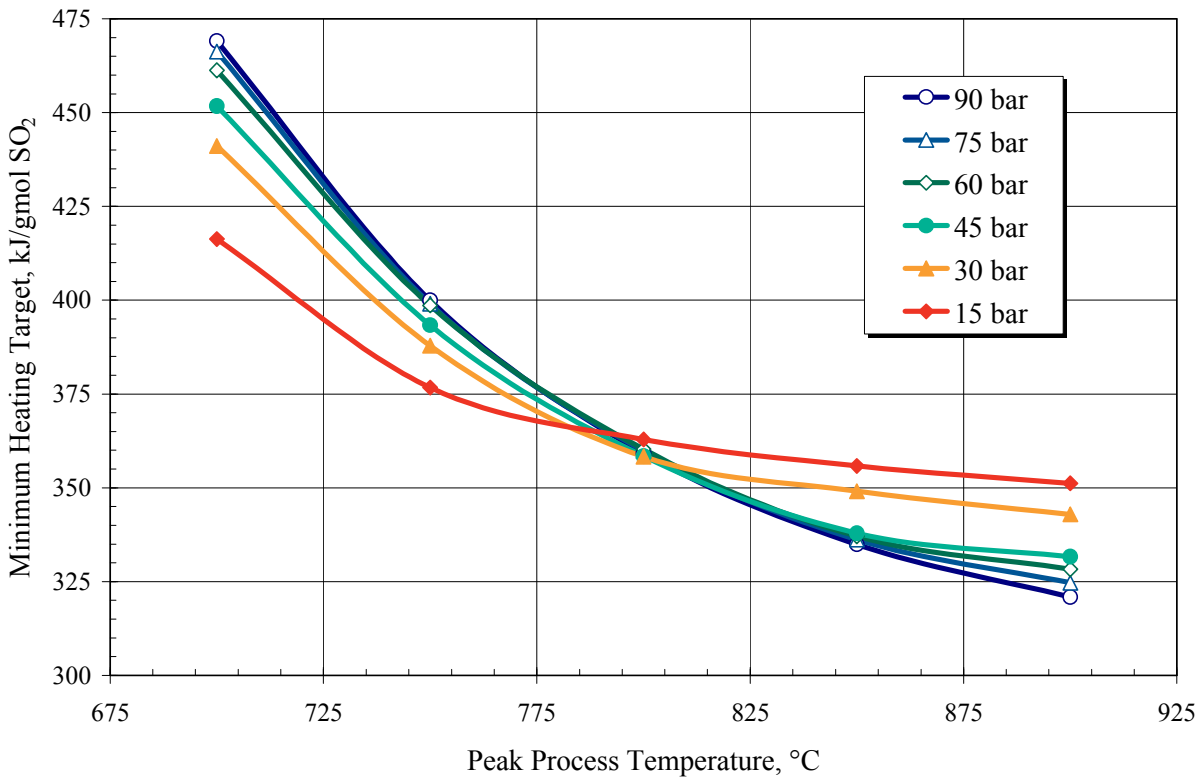

Figure 19.17 Effect of Pressure and Peak Process Temperature on Bayonet Reactor Minimum Heating Target [98]; 80.1 wt% H_2SO_4 Feed Concentration, 675°C Catalyst Bed Inlet Temperature, Thermodynamic Equilibrium in Catalyst Bed, 10°C Minimum Temperature Difference for Recuperation.

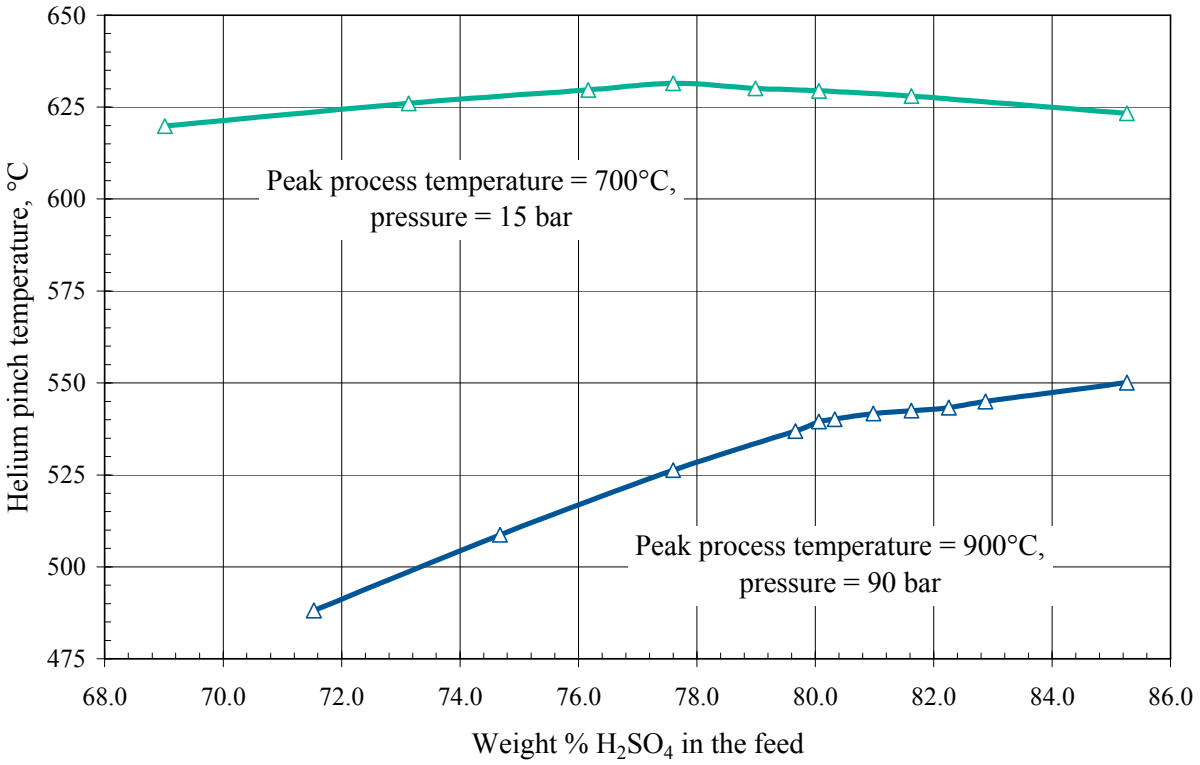

Figure 19.18 Bayonet Reactor Helium Heating Pinch Temperature Dependence on Feed Concentration at Stated Conditions [98]; 675°C Catalyst Bed Inlet Temperature, Thermodynamic Equilibrium in Catalyst Bed, 10°C Minimum Temperature Difference for Recuperation.

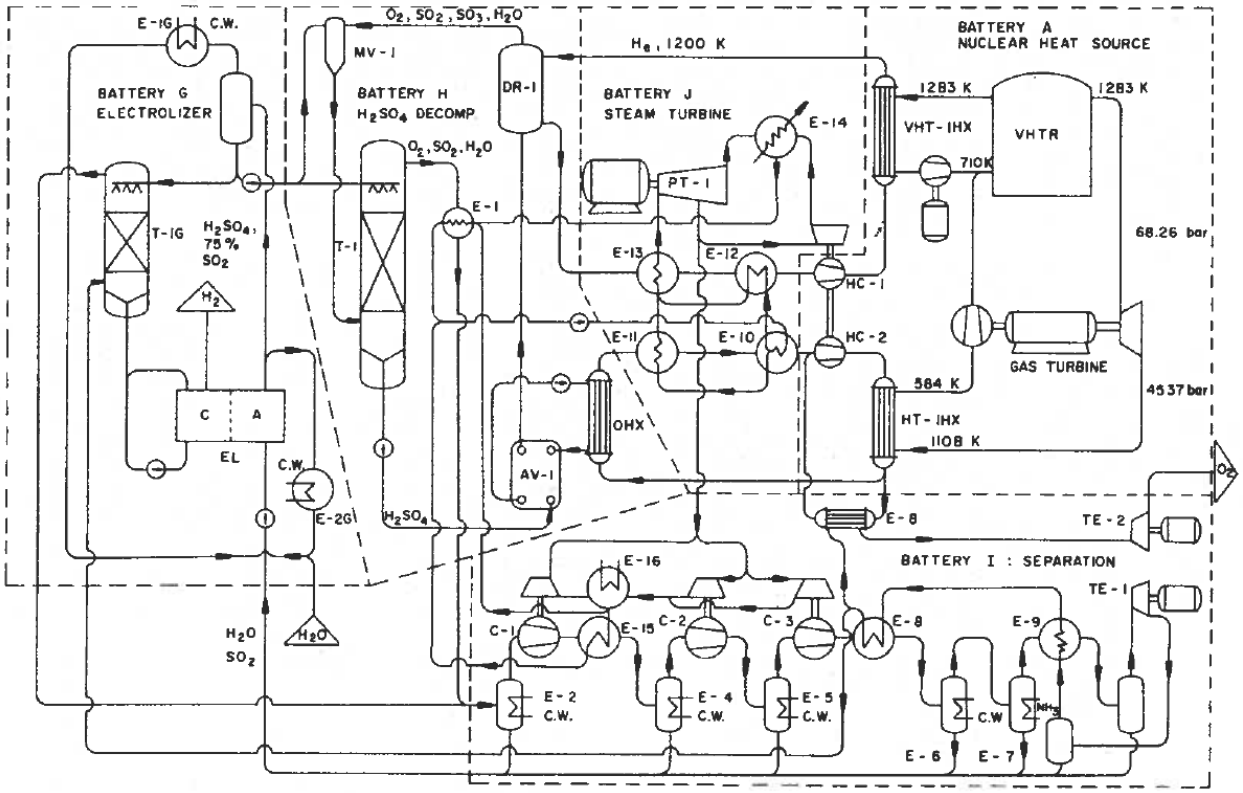

Figure 19.19 Early Westinghouse HyS Flowsheet with Microporous Diaphragm SDE and Low-temperature (-100°C) SO_2-O_2 Separation [58].

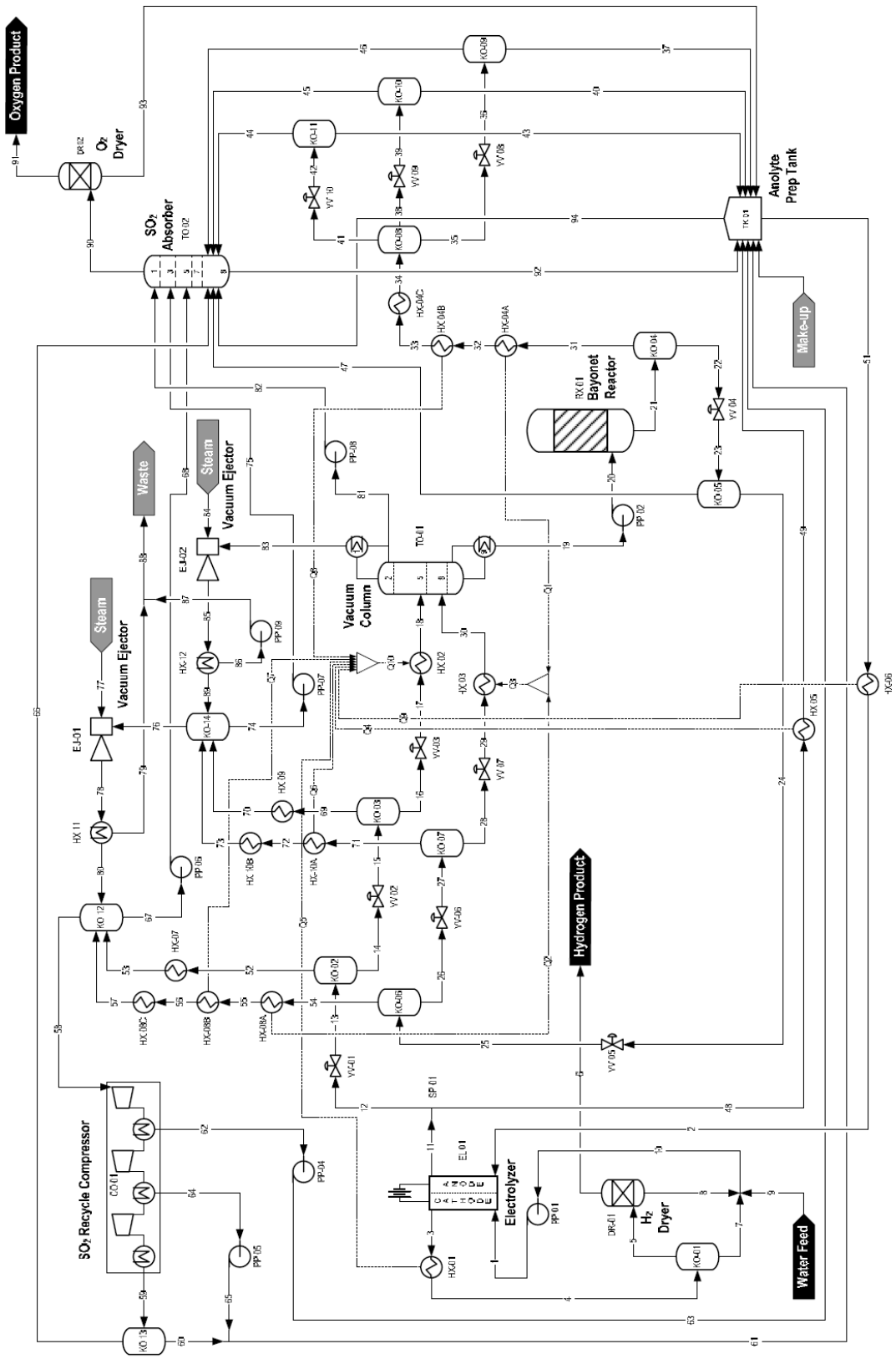

Figure 19.20 HyS Flowsheet Using a PEM SDE and a Bayonet Decomposition Reactor [97].

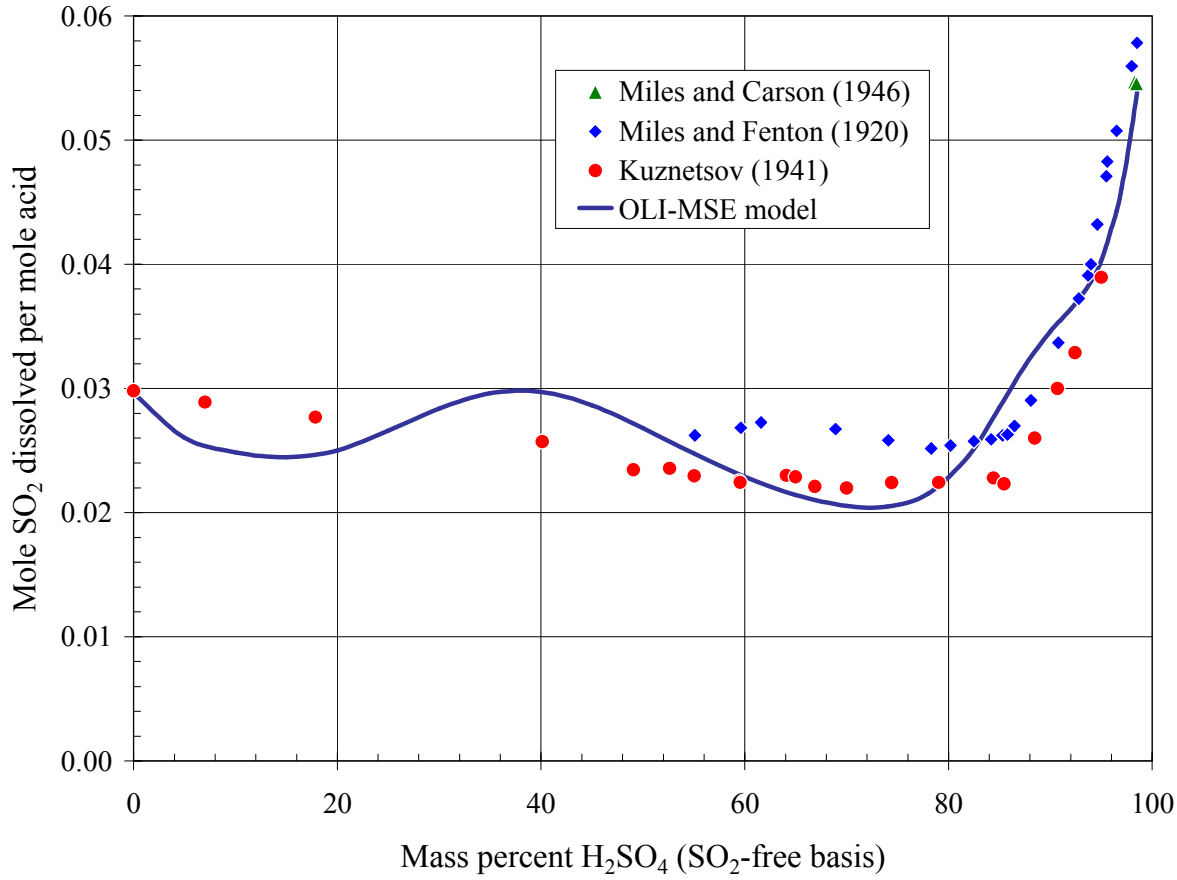

Figure 19.21 Solubility of SO_2 in Sulfuric Acid at 1.013 bar Partial Pressure – Comparison of OLI MSE Model with Data of Miles and Carson [127], Kuznetsov [126], and Miles and Fenton [125] (from Reference [95]).

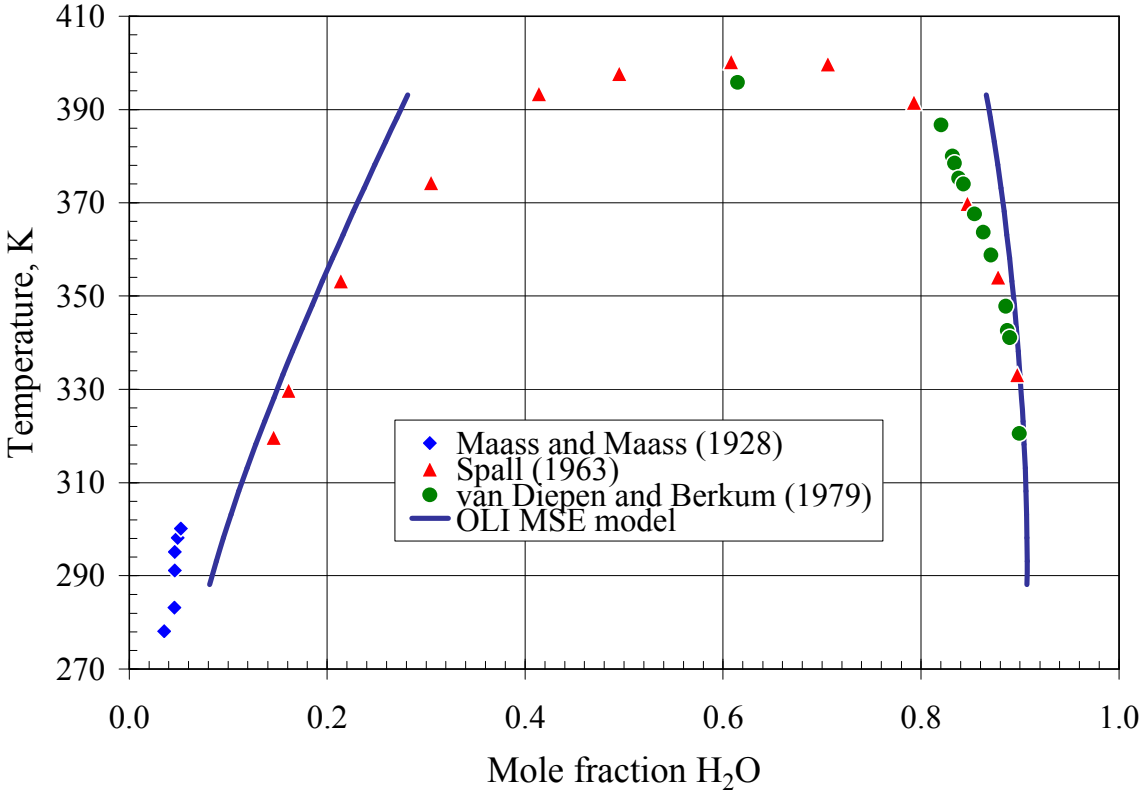

Figure 19.22 Liquid-liquid Phase Equilibrium in the SO_2-H_2O System – Comparison of OLI MSE Model with Data of Maass and Maass [128], Spall [129], and van Diepen and Berkum [130] (from Reference [95]).

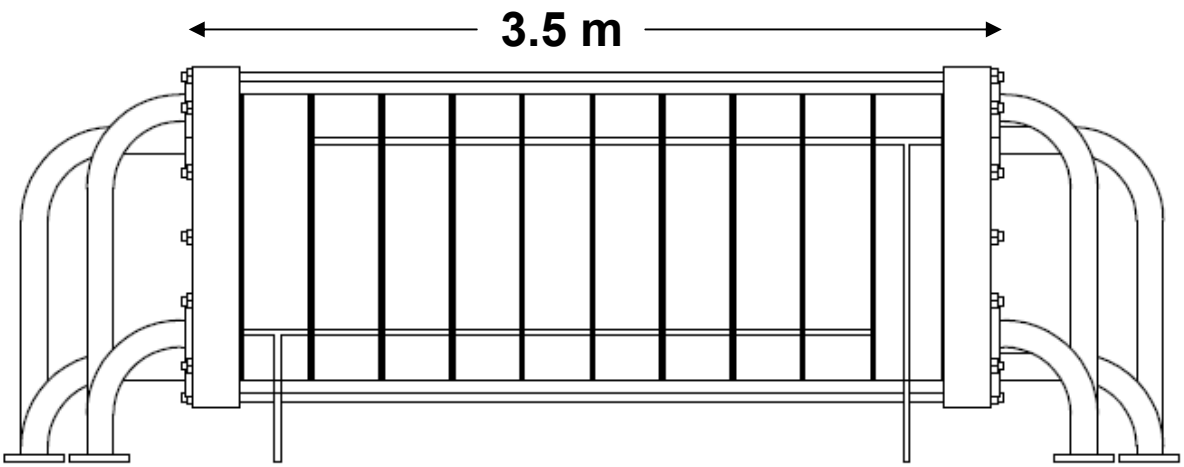

Figure 19.23 Commercial SDE Module Employing 200 Cells of 1-m^2 Active Area Each. Rated Hydrogen Production Rate of 1.5 MW (HHV).

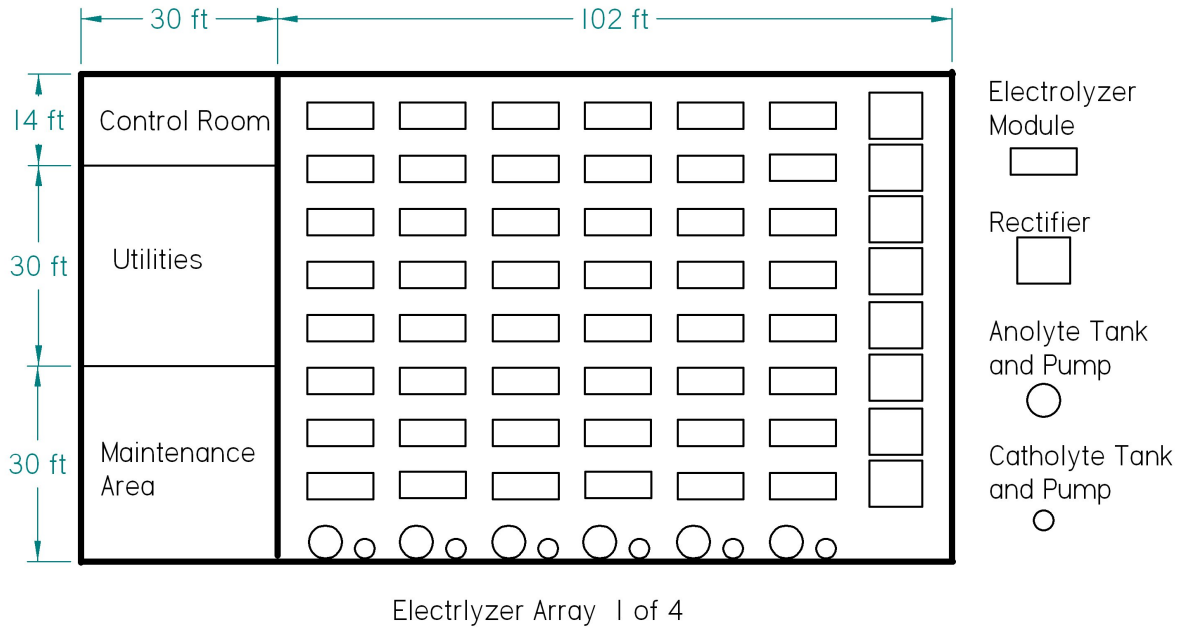

Figure 19.24 Plot Plan of SDE Cell Room Comprising 48 SDE Modules Rated at 1.5 MW of Hydrogen Output Each.

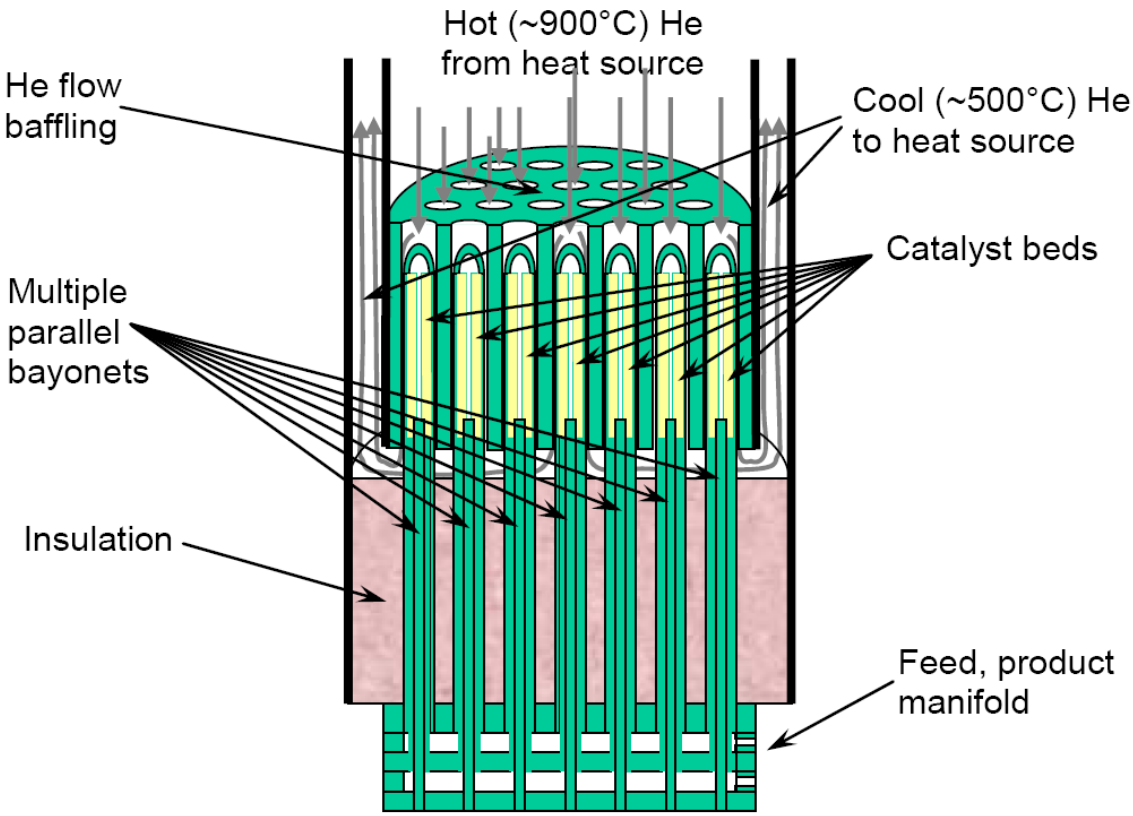

Size: 100 MW_{th}; 3300 tubes; Overall diameter = 5.5 m

Figure 19.25 Commercial-scale Acid Decomposer of Bayonet Design [98].